Geometry and Quaternary kinematics of fold-and-thrust units of southwestern Taiwan

Olivier Lacombe, F. Mouthereau, B. Deffontaines, J. Angelier, H. T. Chu, C. T. Lee

TECTONICS, VOL. 18, NO. 6, PAGES 1198-1223 DECEMBER 1999

Geometry and Quaternary kinematics of fold-and-thrust units of southwestern Taiwan

O. Lacombe, F. Mouthereau, B. Deffontaines, and J. Angelier

Département de Géotectonique, Université Pierre et Marie Curie, Paris

H. T. Chu

Central Geological Survey, Ministry of Economic Affairs, Taipei

C. T. Lee

Institute of Applied Geology, National Central University, Chungli

Abstract. Structural and paleostress analyses provide new insights into the Quaternary kinematics of the outermost fold-and-thrust units of southwestern Taiwan Foothills. The frontal folds are interpreted as fault-related folds, and their tectonic evolution through space and time is tightly constrained. Fold development is correlated with reef building on top of the anticlines. Moreover, we provide field evidence that NW-SE fault zones oblique to the structural grain of the belt probably acted as transfer fault zones during the the Quaternary fold-thrust emplacement. Two successive Quaternary stress regimes are evidenced in southwestern Taiwan: A NW-SE compression, followed by a recent nearly E-W compression. The latter shows an along-strike change from pure E-W contraction to the north to perpendicular N-S extension in the south. This southward decrease in N-S confinement probably represents the on-land signature of the incipient Quaternary tectonic escape predicted by analogue and numerical modelling and evidenced at present-day by Global Positioning System data.

1. Introduction

Arc-continent collision is occurring in the Taiwan segment of the active convergent plate boundary between the Philippine Sea plate and Eurasia [*Suppe*, 1984; *Ho*, 1986a, b; *Barrier and Angelier*, 1986; *Angelier et al.*, 1986, 1990; *Teng*, 1990]. This collision segment connects the south verging Ryukyu subduction zone, where the Philippine Sea Plate is subducting beneath the Eurasian Plate, and the west verging Manila subduction zone, where the Philippine Sea Plate is overriding the crust of the South China Sea (Figure 1). The orogen which developed in Taiwan during the late Cenozoic, mainly since 5 Ma [*Ho*, 1986a, b], is consequent to this collision between the Luzon arc and the Chinese passive margin.

Because of the obliquity of the convergence between the Philippine Sea Plate and the Eurasian Plate, subduction within the Manila trench evolves northward into incipient collision south of Taiwan, near the transition between oceanic and continental crust within the subducting Eurasian lithosphere; active collision culminates on-land within the southwestern part of the island (Figure 1). The northern part of Taiwan was deforming until recent times but is presently less active because of the southward propagation of the collision through time.

In this paper, we focus on the geometry and kinematics of the outermost units of the southwestern Taiwan Foothills: This is the key region to understand how the offshore Manila subduction and related accretionary wedge evolves northward to the oblique collision prevailing in southwestern Taiwan (Figure 1). Our aim is to provide a complete structural map of southwestern Taiwan and to discuss the geometry and kinematics of tectonic features related to the collision. For this purpose, structural analyses were carried out on the basis of subsurface data, satellite imagery, digital elevation models and fieldwork. Paleostress reconstructions were performed in order to define the orientation of the tectonic forces responsible for mountain building in the area investigated and to constrain both the tectonic mechanisms prevailing during the Quaternary and the kinematics of the westward propagating units.

2. Sedimentary and Structural Setting

The investigated area of southwestern Taiwan corresponds to the southern part of a Plio-Pleistocene foreland basin which developed in response to lithospheric flexure due to the tectonic loading of the Central Range orogenic belt. The nearly 5 km thick sediments of the foredeep consist of Pliocene bathyal to shallow marine and Pleistocene neritic to fluvial deposits; they unconformably overlie the precollisional Miocene shelf to bathyal deposits of the Chinese passive margin. These formations were deformed and partially exposed because of the westward propagation of the collision: They are deformed by stacked west vergent folds and thrust sheets resulting from the late Cenozoic collisional shortening. This deformation decreases toward the still slightly deformed but progressively deforming western Coastal Plain, where the Pleistocene formations are generally unconformably overlain by Holocene terrace deposits.

Paper number 1999TC900036.
0278-7407/99/1999TC900036$12.00

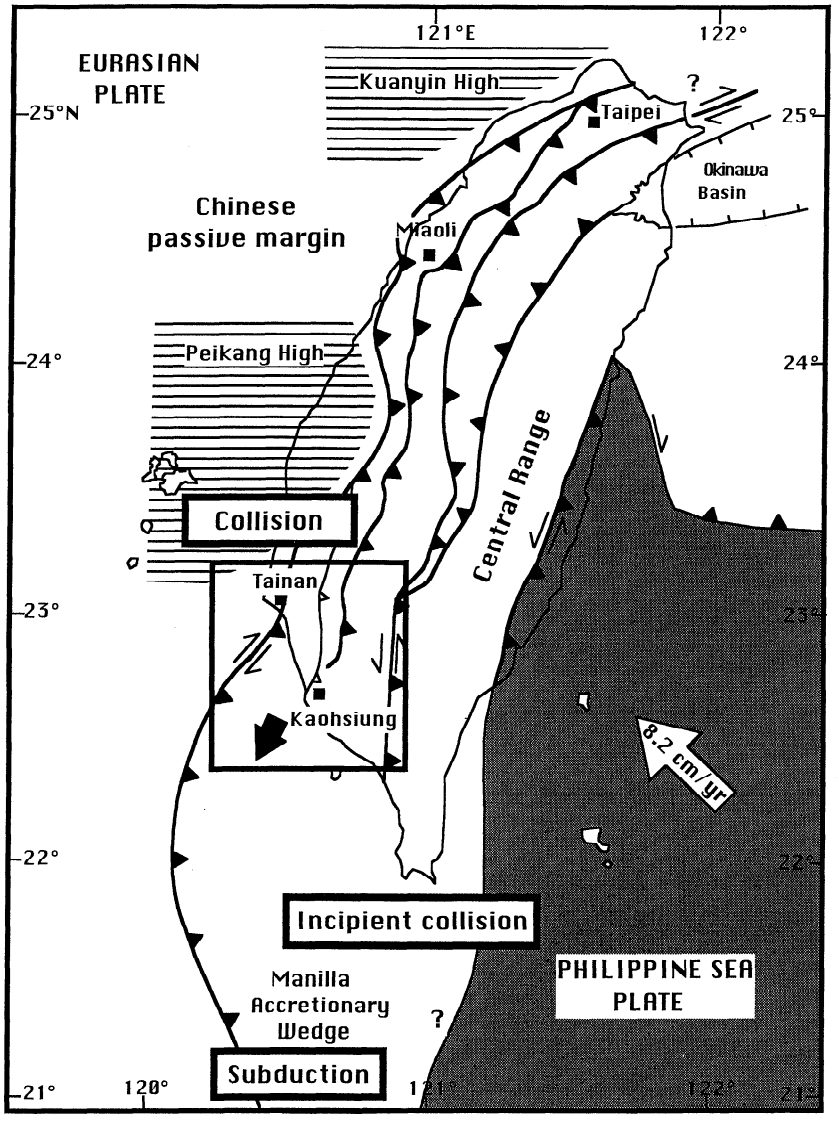

Figure 1. Geotectonic setting and main structural features of Taiwan. The large open arrow shows the present direction of convergence of the Philippine Sea Plate (shaded) relative to south China; velocity is after *Yu et al.*, [1997]. Heavy lines indicate major thrusts; triangles are on upthrown side. Hatched areas correspond to basement highs of the Chinese margin which underlie the deposits of the foreland basin. The frame indicates the location of the area investigated.

Most of the formations cropping out in the study area are thus detritic deposits of late Pliocene-Pleistocene age; they correspond to the sedimentary record of the collision. Precollisional Miocene formations may locally be found at the surface but only in the vicinity of major thrusts (Figure 2). In the northern part of our study region (domain 1, Figure 2), the late Pliocene lithostratigraphic units consist of the Chutouchi Formation (Nannoplankton Zones: NN15-NN17) and the overlying Liuchungchi Formation (NN18), made of sandy shales and muddy sandstones (Figure 3, column A). These late Pliocene formations are overlain by the Pleistocene formations, which are, from base to top, the Kanhsialiao and the Erchungchi Formations (NN19), mainly composed of interbedded shales and sandstones, and the Liushuang Formation (NN20), composed mostly of gray mudstones and shales [*Ho*, 1986a, b].

In contrast, the late Pliocene-Pleistocene formations in the southern Tainan-Kaohsiung area (domain 2, Figure 2) mainly consist of the thick Gutingkeng Formation, ranging in age from NN13 to NN19 (Figure 3, column B). It is mostly composed of dark gray mudstones interbedded with thin bedded sandstones. It is generally overlain by the Liushuang and the Erchungchi Formations. The upper Gutingkeng Formation, the Erchungchi Formation, and the lower Liushuang Formation change laterally to the southeast (Figure 3, column C) to the NN19-NN20 Lingkou Conglomerate, which locally may directly overlie the NN14 Nanshihlun Formation. The lateral changes in facies and thickness between these formations as

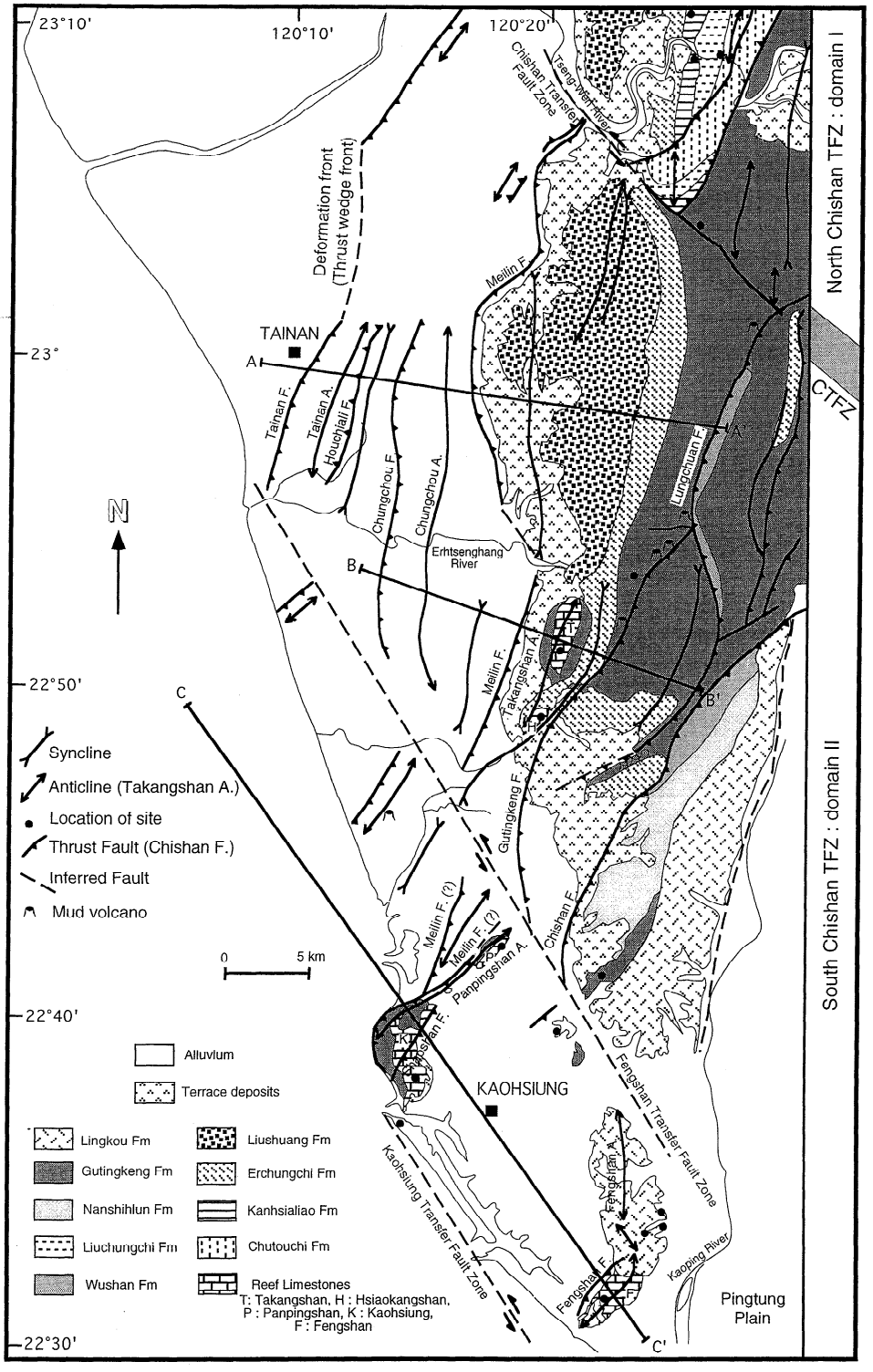

Figure 2. Structural map of southwestern Taiwan (*Chinese Petroleum Corporation*, [1974] and this work). The investigated area is divided into a domain 1, north of the Chishan Transfer Fault Zone (CTFZ)(outlined by the shaded area on the right), and a domain 2, south of it. See Figure 3 for thickness of sedimentary formations and time correlations. The names of major faults and anticlines used in the text and in the sections of Figure 5 are reported. Note the transverse fault zones (dashed lines) which are interpreted as transfer fault zones. A-A', B-B', and C-C' show location of cross sections of Figure 5.

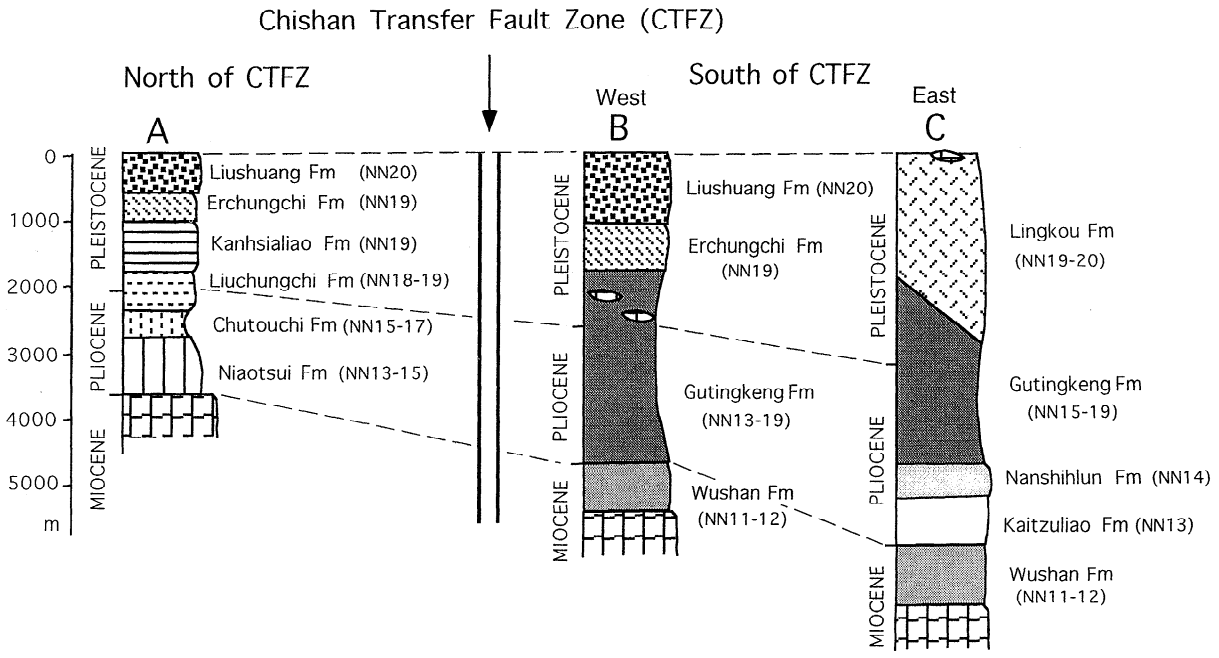

Figure 3. Stratigraphic columns showing time correlations between Neogene sedimentary formations in southwestern Taiwan. Ages are after *Chinese Petroleum Corporation*, [1974], *Chi*, [1979], *Chang and Chi*, [1983], *Ho*, [1986a, b], *Chi*, [1989], *Lee*, [1990], *Lin*, [1991], *Gong et al.*, [1996]. Column A is located north of the CTFZ; columns B and C are south of it. Note the lateral variations of type and thickness of formations across the CTFZ, as well from NW to SE south of it (columns B and C). The patterns are the same as those in Figure 2. Note the lenses of reef limestones (see Figure 2 for localities).

well as their local conformable or unconformable attitude with respect to the underlying ones reflect the dynamics of the foredeep basin with depocenters changing in space and time in response to the westward propagation of thrust units and the southward migration of the collision.

Reef limestones are distributed sparsely in the Pleistocene rocks of southwestern Taiwan [*Ho*, 1986a, b]. These limestone lenses vary from several meters to nearly 100 m in thickness and from 10 m to several thousand meters in length; they often thin out laterally over short distances and grade into the poorly stratified muddy sediments (Figure 3). The main reef localities are Takangshan, Hsiaokangshan, Panpingshan, Kaohsiung, and Fengshan (Figure 2). For instance, the NN19 Kaohsiung limestone is nearly 300 m thick and mainly composed of corals, bryozoairs, foraminifera, molluscs, and numerous thin mudstone layers; the NN20 Fengshan limestone is composed of gray coral reef limestone, with a total thickness of nearly 30 m. These recently uplifted limestones provide a very suitable material for analyzing brittle deformation.

3. Methods Used in Structural Analysis

Our structural analysis of the tectonic features of the Foothills of southwestern Taiwan combines fieldwork, new interpretations of already published structural data, and morphostructural studies. The occurrence, geometry, and mechanism of major features inferred from morphological and remote-sensing data (Figure 4) were checked and characterized in the field, and these new data were used to improve the regional structural mapping (Figure 2). Geological cross sections constrained by drill holes and seismic profiles where available (Chinese Petroleum Corporation, unpublished data, 1997) describe the geometry at depth of frontal fold-and-thrust units (Figure 5). Finally, tectonic analyses based on fault slip data and calcite twin data reveal the Quaternary stress patterns and bring constraints on the kinematics of propagating units. These methods are briefly summarized in sections 3.1-3.3.

3.1. Digital Elevation Model (DEM) and SPOT-Panchromatic Image Analysis

Because the recent age of deformation in Taiwan makes possible a rather good correlation between tectonics and morphology, we carried out a study of a digital elevation model (DEM) of southwestern Taiwan in order to decipher structural information through the outermost geomorphological features of the Foothills. Such data were obtained by numerical autocorrelation of aerial photographs of the western Foothills of Taiwan. The ground resolution of the DEM presented in Figure 4a is 40x40 m. This analysis provides additional information with respect to previous subsurface data and photogeologic interpretations [*Sun*, 1963, 1964].

Two types of major features could be recognized. The first type consists of features striking parallel to the belt; most of them correspond to major anticlines and thrusts (Figure 4b). The second type of features strikes obliquely to the structural grain of the belt. Where lithological contrasts are absent and thus cannot account for differential erosion, these transverse features correspond to fault zones [*Deffontaines et al.*, 1994]. Additional field studies (this work) resulted in identification of

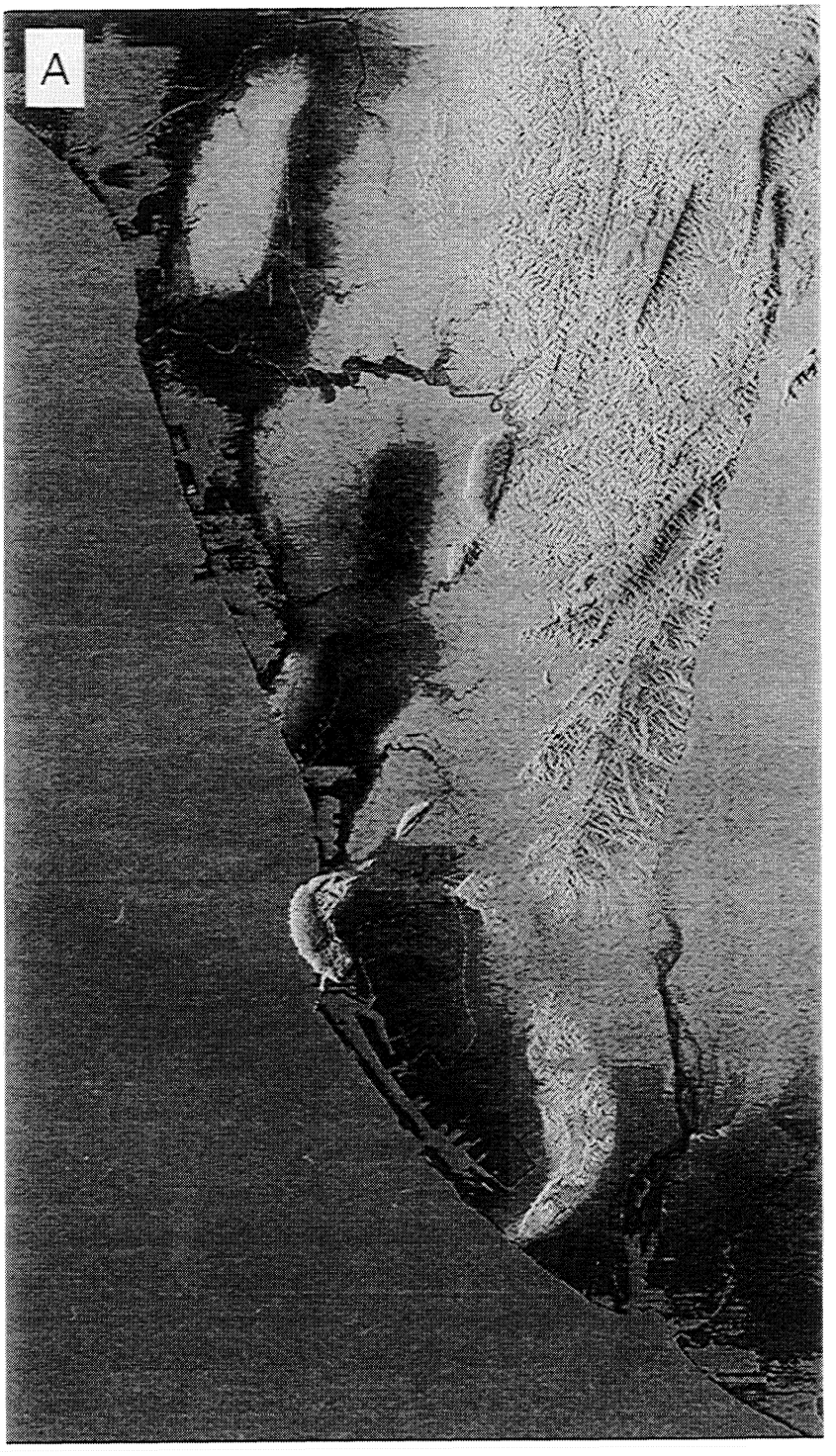

Figure 4. (a) Digital elevation model of southwestern Taiwan. (b) Structural interpretation of morphologic features.

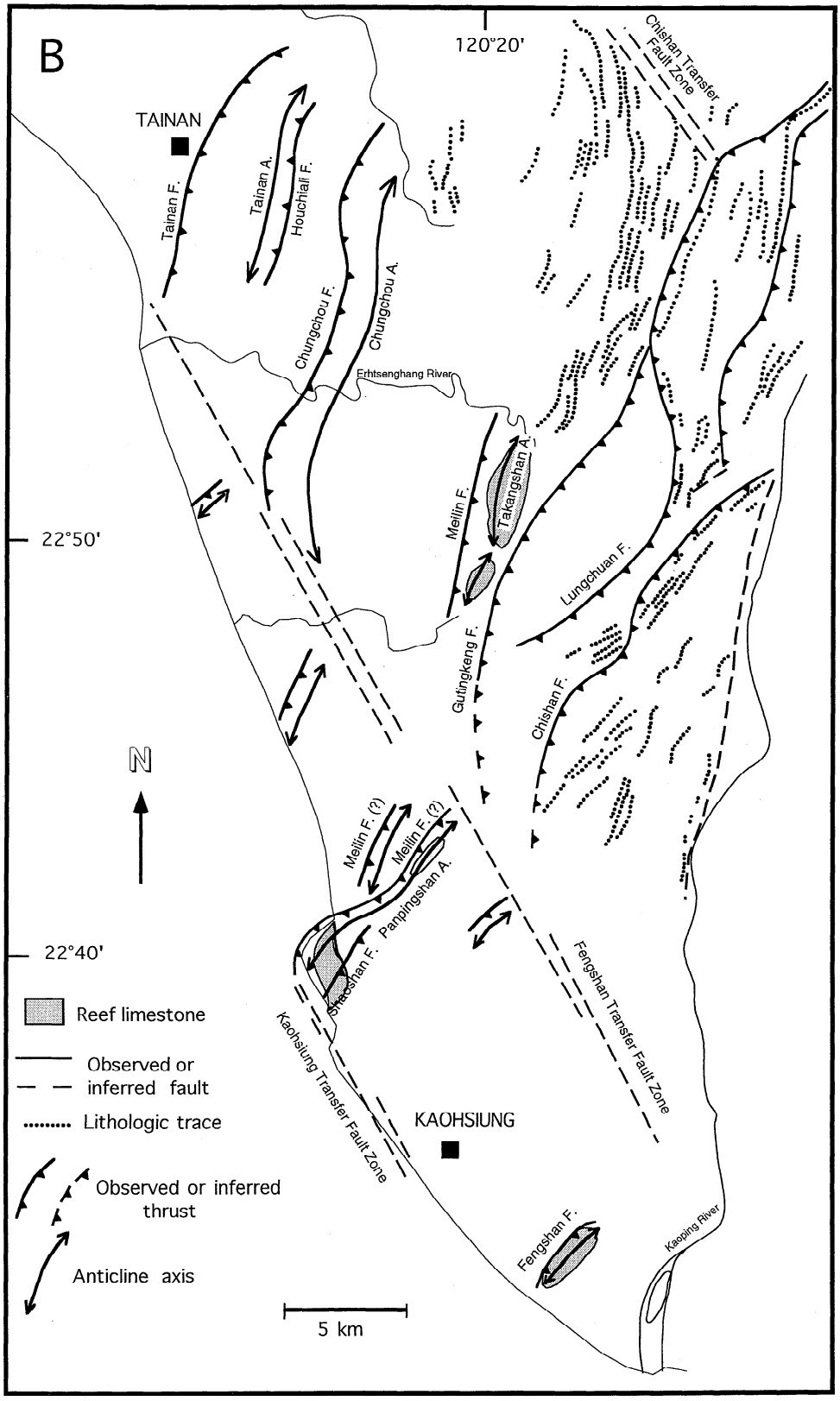

Figure 4. (continued)

major and minor fracture sets along such oblique trends, and brought constraints on both their kinematics and tectonic significance.

These geomorphological studies were complemented by interpretations of high-resolution SPOT panchromatic scenes (10x10 m ground resolution) of western Taiwan. Both analyses allow improvement of the structural information reported on previous geological maps [Chinese Petroleum Corporation, 1974; *Ho*, 1986a, b](Figure 2).

3.2. Construction of Geological Cross Sections

Three geological cross sections were constructed perpendicular to the outermost fold-and-thrust units (Figure 5). The control at depth of these sections was provided by well data (location on cross sections) and seismic profiles (Chinese Petroleum Corporation, unpublished data, 1997) where available. The Plio-Pleistocene synorogenic deposits provide time constraints on the structural evolution of the units. As discussed in sections 4.2.1-4.2.3, these cross sections highlight the geometry, extension at depth, and spacing of fold-thrust systems and the lateral changes in thickness and type of sedimentary formations. They provide evidence for the regional along-strike change in kinematics and structural style of the deformed units. At a more local scale they highlight the close relationships between reefs and fault-related folds (Figure 5).

3.3 Paleostress Analyses

The analysis of macrostructures was combined with a detailed study of small-scale brittle deformation, such as striated microfault surfaces, stylolites, joints, and tension gashes. The location of sites is reported in Figure 2. The dynamic interpretation of these microstructures in terms of tectonic stress patterns brought constraints on both the Quaternary tectonic mechanisms and the kinematics of propagating units.

Computation of paleostress tensors was performed on the basis of inversion of fault slip data [*Angelier*, 1984]. The basic principle consists of finding the best fit between the observed directions and senses of slip on numerous faults and the theoretical shear stress induced on these planes by the tensor solution of the inverse problem. The results are the orientation (trend and plunge) of the three principal stress axes σ_1, σ_2, and σ_3 (with $\sigma_1 \geq \sigma_2 \geq \sigma_3$, pression considered positive) and the Φ ratio between differential stress magnitudes ($\Phi=(\sigma_2-\sigma_3)/(\sigma_1-\sigma_3)$, with $0\leq\Phi\leq1$). Additional information is obtained from stylolites, tension gashes, and joints. The procedure for separating successive stress tensors and related subsets of fault slip data is based on both mechanical reasoning [e.g., *Angelier*, 1984] and relative tectonic chronology data (superimposed striations on fault surfaces, crosscutting relationships between faults, ...).

In order to establish a time distribution of tectonic regimes, dating of the brittle structures also requires stratigraphic information about the age of the deformed units and/or evidence of syndepositional tectonism. Particular attention was also paid to rotations of rock masses due to folding. Reconstruction of the original attitudes of minor structures and related paleostress axes with respect to fold axes and bedding attitudes was thus performed in the following way: Where tilted bedding is observed as a result of folding, several cases deserve consideration, because faults may have formed before, during or after folding. Following *Anderson* [1951], we assumed that one of the three principal stress axes of a tensor is generally vertical. If a fault set formed before folding and was secondarily tilted with the bedding, the tensor calculated on this set does not display a vertical axis. Instead, one of the stress axes is generally found perpendicular to bedding, whereas the two others lie within the bedding plane. Accordingly, the conjugate fault systems do not display vertical planes of symmetry. In such a case, it is necessary to back tilt the whole system (faults, tensor, and bedding) in order to put it back in its initial position. Within a heterogeneous fault population this geometrical reasoning allows separation of data subsets based on their age relative to fold development. For simplicity we only provide examples of the most significant diagrams illustrating fault slip data. The corresponding stress tensors are listed in Table 1.

The reef limestones also provide a suitable material for paleostress reconstructions based on inversion of mechanical twins in calcite [*Etchecopar*, 1984; *Laurent*, 1984]. They contain large sparry calcite crystals resulting from recrystallization during diagenesis of the primary aragonitic material and micritic calcite. These sparry grains are of nearly homogeneous size and developed independently with respect to the initial organic network (Figure 6); they display nearly random crystallographic orientations, which is appropriate for calcite twin analysis. Twin lamellae within these grains are straight and narrow, indicating low strain (less than 2 or 3%) and low temperature (<200°C). Paleostress reconstructions were thus carried out on the basis of inversion of mechanical calcite twin data [*Lacombe et al.*, 1993; *Rocher et al.*, 1996; this work].

4. Geometry and Kinematics of Fold-and-Thrust Units

The study area is limited to the north by an oblique fault zone, the Chishan Transfer Fault Zone (CTFZ) [*Deffontaines et al.*, 1997] (Figure 2), whose tectonic significance will be discussed in section 5. This oblique fault zone corresponds to the surface expression of a broader transition area underlined by numerous earthquakes (some of them as deep as 80 km [*Wu et al.*, 1997]) which clearly separates a northern domain (domain 1 in Figure 2) in front of the Peikang High, which displays high seismic activity, and a southern region (domain 2 in Figure 2) where shallow (between 0 and 20-25 km depth) earthquakes are scarce [*Wu et al.*, 1997]. This zone corresponds to the transition between a northern region where collision is taking place and involves the deformation of the continental basement (and the whole crust [*Wu et al.*, 1997]), and a southern region which can be described as the on-land extension of the Manila accretionary wedge, where shortening occurs while the deformation front moves westward toward the Eurasiatic continental shelf. From structural and sedimentary points of view this zone is also marked by an important lateral variation in type and thickness of sedimentary formations (Figure 3) as well as contrasting styles of deformation [*Mouthereau et al.*, 1999a, b].

In this paper, we focus on the southern region, but we briefly present the results of tectonic analyses carried out just north and along the surface trace of the so-called Chishan Transfer Fault Zone, in order to allow comparison with the southern area. For the sake of simplicity, sections 4.1-4.2 report separately the results obtained in the two subregions located north and south of the CTFZ, respectively (domains 1 and 2 in Figure 2).

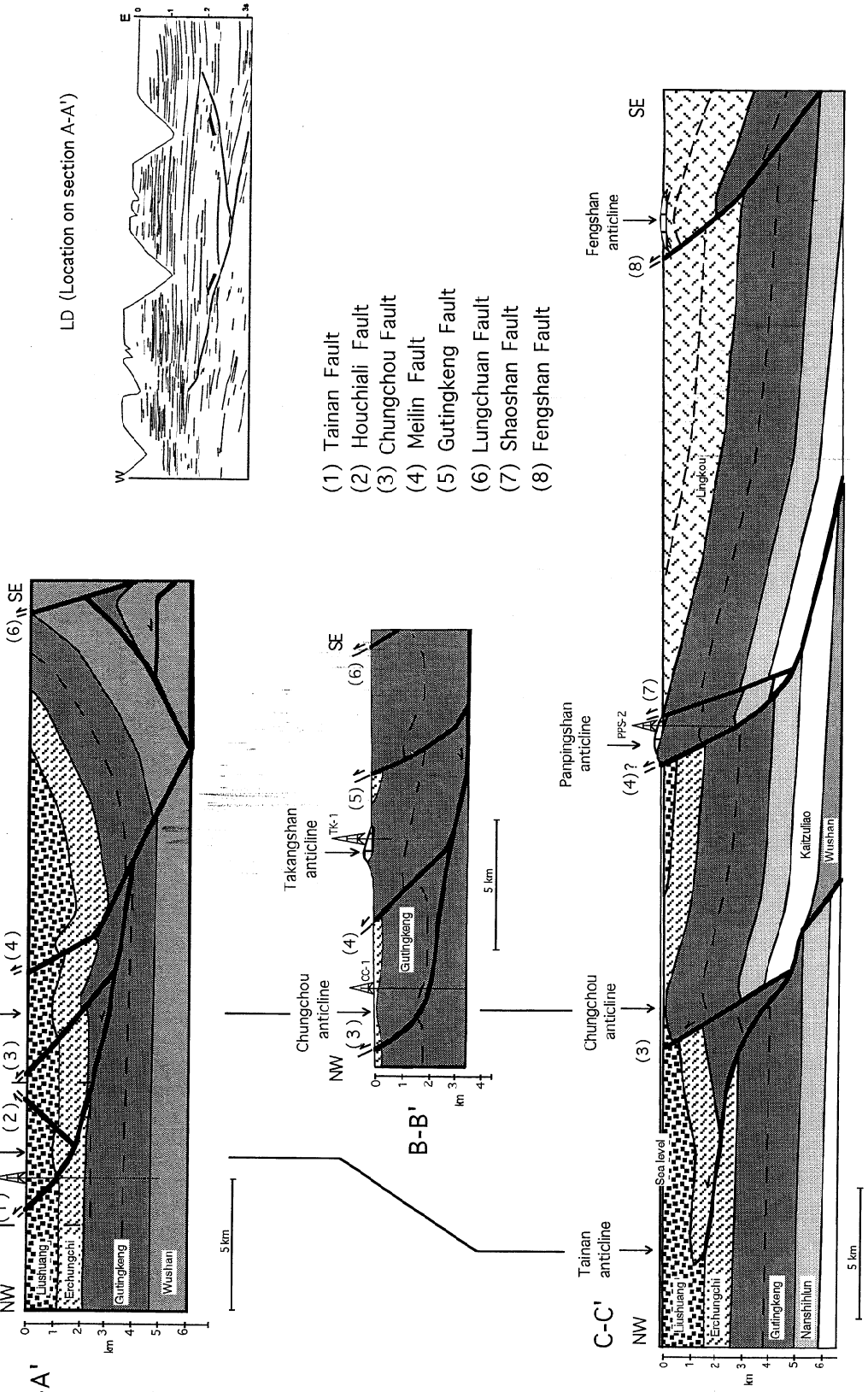

Figure 5. Geological cross sections through the area investigated (location in Figure 2), constrained by well data (projected on the sections) and seismic lines. The patterns used for sedimentary formations are the same as those used for the map of Figure 2 and the stratigraphic columns of Figure 3. The Holocene formations have not been represented. Note the particular location of the reefs and the fault-propagation fold geometry. LD, Line drawing (upper right), located on section A-A'. In the offshore part of section C-C', the Tainan and Chungchou anticlines have been extrapolated. The numbers refer to faults located in Figure 2.

Table 1. Results of Stress Tensor Determination Based on Fault Slip Data

Site	Diagram	Trend (Plunge) of the Principal Stress Axes			Ratio Between Differential Stresses	Total Number of Faults	Quality of Tensor
		σ_1	σ_2	σ_3	(Φ)	(F)	(Q)
1	b*	092 (27)	325 (38)	207 (30)	0.3	6	c
	c*	085 (01)	355 (19)	178 (71)	0.3	22	a
	d*	089 (08)	358 (06)	233 (81)	0.2	11	a
2	*	107 (17)	231 (62)	010 (22)	0.4	7	c
3		287 (16)	080 (72)	194 (08)	0.2	6	c
4	a*	111 (16)	300 (74)	202 (02)	0.2	22	a
	b*	082 (03)	288 (87)	172 (02)	0.4	46	a
5	a	274 (03)	037 (84)	183 (05)	0.1	89	a
	b	127 (17)	324 (72)	218 (05)	0.5	23	a
	c	288 (74)	066 (12)	158 (10)	0.2	9	a
6	a	270 (04)	029 (81)	179 (08)	0.1	46	a
	b	148 (70)	016 (14)	283 (03)	0.3	5	b
7	a	334 (72)	236 (03)	145 (18)	0.4	11	a
	b	132 (02)	011 (87)	222 (03)	0.0	30	a
8	a	131 (03)	338 (87)	221 (02)	0.3	36	a
	b	025 (69)	192 (21)	284 (04)	0.2	22	a
	c	073 (03)	306 (85)	164 (04)	0.2	13	b
9		302 (03)	184 (85)	033 (05)	0.4	34	a
10		111 (11)	229 (66)	017 (20)	0.2	13	b
13	b	254 (80)	084 (10)	354 (02)	0.4	12	a
14	a	170 (76)	022 (12)	291 (07)	0.3	6	c
	b	188 (88)	083 (01)	353 (02)	0.3	22	a
	c	305 (02)	208 (76)	035 (12)	0.2	10	b
15	b	290 (01)	033 (86)	200 (04)	0.5	19	b

Trend and plunge of each stress axis are given in degrees. Ratio Φ is defined in text. F, number of faults consistent with the tensor; and Q, quality of the tensor (a to c) estimated according to the number of faults explained, the variety of their orientations, and intraprogram numerical quality estimators [*Angelier*, 1984].

* Back tilted stress axes.

4.1. Area North of the Chishan Transfer Fault Zone (Domain 1 in Figure 2)

Immediately north of the CTFZ (Figure 2), Pleistocene mudstones display steep dips to the west as a consequence of the development of NNE trending folds and thrusts (Figure 7). At the outcrop scale, brittle features reveal a dominating nearly E-W compression. Three main types of fracture sets could be observed in this area.

The first set consists of subvertical E-W trending tension joints (Figure 7, diagram a at site 1), consistent with a mean E-W compression. The second type includes N140°-160°E left-lateral strike-slip faults and N70°E right-lateral ones. The striations are often non horizontal and parallel with the bedding. We infer that these strike-slip faults developed before folding and were secondarily tilted. Such patterns should therefore be analyzed in their initial attitude. Thus bedding was back tilted along the local strike of beds (because the folds are generally cylindric), which allowed restoration of the original attitude of fault patterns (e.g., Figure 7, diagram b at site 1 and diagram at site 2). In contrast, some strike-slip faults exhibit nearly horizontal striae oblique to tilted bedding (Figure 7, diagram at site 3) and should thus be interpreted as faults which developed after folding. The third type of brittle structures consists of apparent normal fault patterns, associated with a steeply plunging σ_1 axis, and a shallowly plunging, N80°E trending σ_3 axis. These normal faults do not reflect extension: Backtilting the strata as before restores the initial pattern, a simple system of reverse faults consistent with a subhorizontal E-W compression (Figure 7, diagrams c and d at site 1). This compression is nearly perpendicular to fold axes and similar to that deduced from tension joints and strike-slip faults.

We conclude that a nearly E-W compression accounts for all the tectonic features observed at different scales. Faulting and folding occurring during the same compressional event produce apparently complicated fault patterns; however, the geometrical-mechanical analysis provides a key to identify and interpret these patterns, thus revealing that the stress regimes remained rather constant during folding.

Seismic investigations as well as mapping of the top of the pre-Miocene basement using well data in this northern region emphasize the involvement of the basement in the thrust wedge and the superimposition of shallow décollement and deep-seated décollement tectonics. It is not the aim of this paper to discuss the structural style of this northern area in

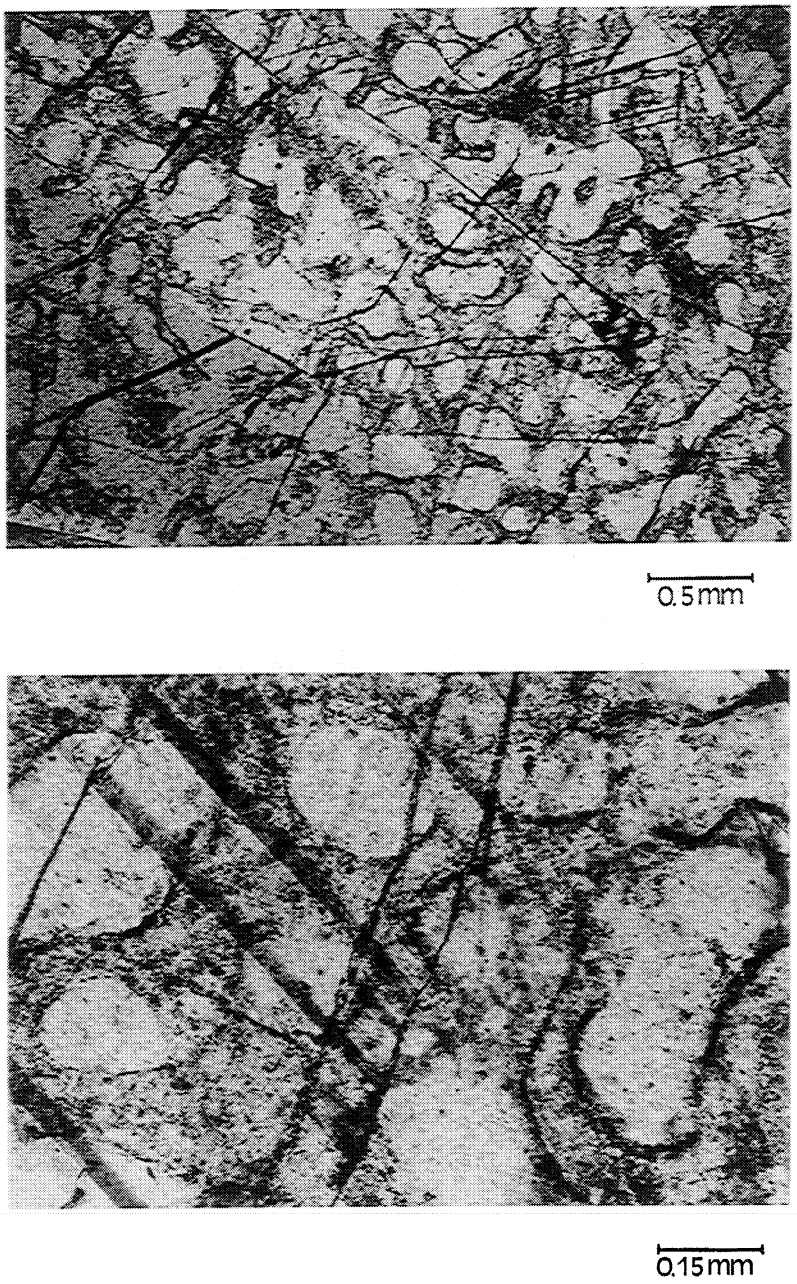

Figure 6. Microphotographs (in natural light) of a coral limestone showing twin lamellae cross cutting sparry calcite crystals resulting from recrystallisation regardless of the initial coralline organic network.

detail (see *Mouthereau et al.* [1999a, b] for cross sections and review of previous works).

4.2. Area South of the Chishan Transfer Fault Zone (Domain 2 in Figure 2)

In contrast to the northern domain, where the basement is involved in collisional shortening [*Mouthereau et al.*, 1999a, b], deformation in the Tainan-Kaohsiung province did not involve the pre-Miocene basement. The propagation of frontal thrust units probably occurred above a low dipping and shallow décollement surface, above the pre-Miocene basement (Figure 5): Structures consist of regularly spaced fault-propagation folds and pop-up structures, which usually develop in relation to flat detachments with low-friction conditions [*Huiqi et al.*, 1992] such as for accretionary wedges. This deformation style is therefore largely controlled by high-fluid-pressure conditions, as shown by the thick poorly consolidated muddy Quaternary deposits and the numerous mud volcanoes (Figure 2). This confirms that this province can be regarded as the onshore extension of the submarine Manila accretionary wedge [*Sun and Liu*, 1993; *Liu et al.*, 1997], so

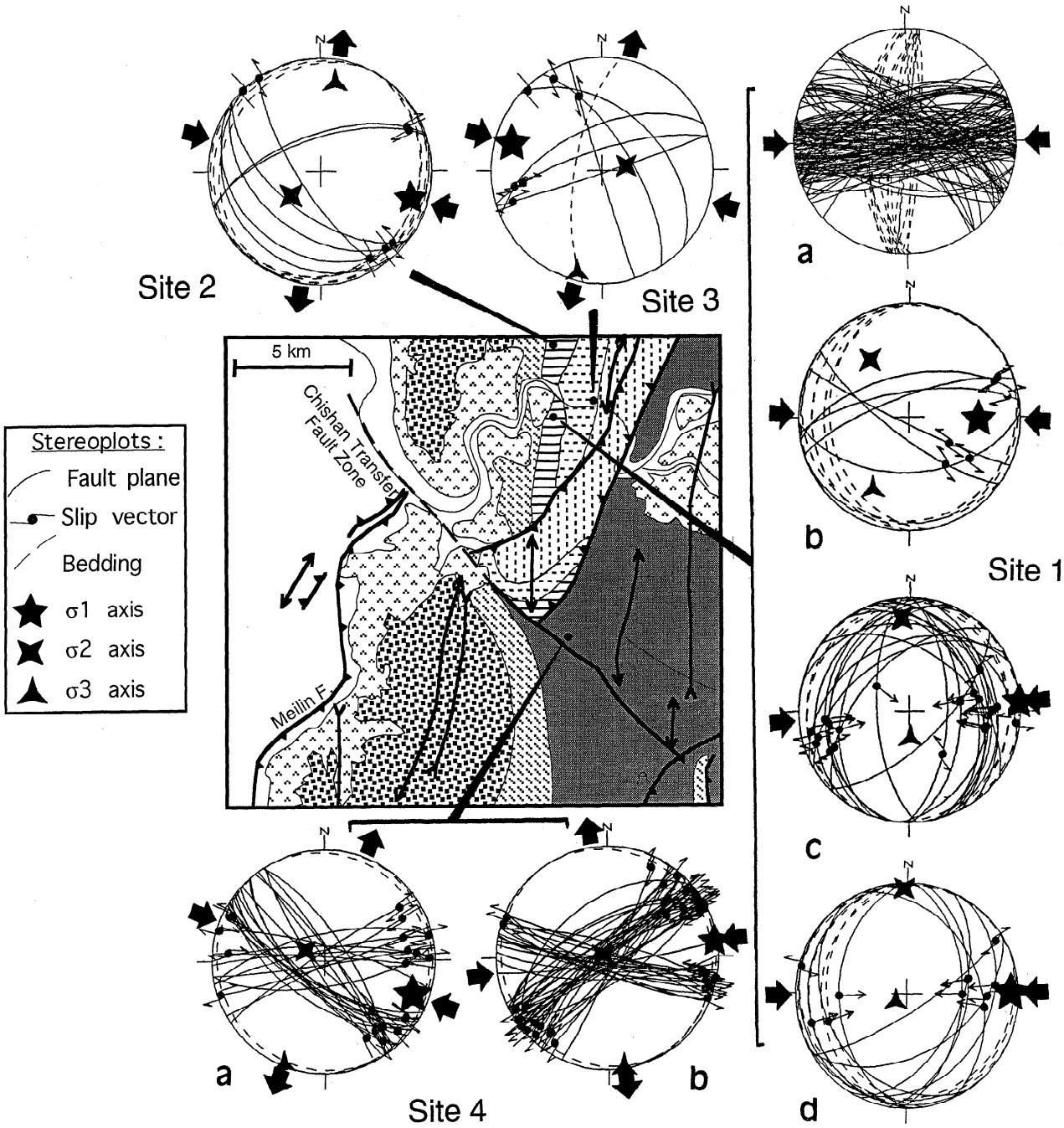

Figure 7. Results of stress reconstruction based on fault slip analysis along and away from the surface trace of the Chishan Transfer Fault Zone.
The map is part of that of Figure 2 (Longitude: 120°20'-120°30'; Latitude: 23°-23°10') and uses the same key. Site numbers refer to sites of Figure 2 and of Table 1.

that the deformation front defined on-land (Figure 2) can be correlated with the offshore northern extension of the Manila trench.

4.2.1. Tainan and Chungchou anticlines. The analysis of the high-resolution DEM of southwestern Coastal Plain of Taiwan (Figure 4) provides evidence of slightly elevated, asymmetric hills, striking parallel to the NE trend of the known folds and thrusts. There is no significant drainage parallel to the NE direction to explain these features in terms of erosion. Therefore we consider that these morphologic features are of tectonic origin and cannot result from erosion solely: They are interpreted as the outermost west vergent folds.

Available well data and seismic reflection profiles (Chinese Petroleum Corporation, unpublished data, personal

communication, 1997) confirm the tectonic origin of these features (Figure 5): In the western part of the A-A' section, two shallow thrust-related folds were identified in the Pleistocene cover (Liushuang-Erchungchi Formations). The Tainan Fault is considered as the outermost thrust and corresponds to the so-called deformation front, which is therefore located farther NW than in previous locations (e.g., near Kaohsiung according to *Lee et al.* [1995]). The Tainan thrust (and the Houchiali backthrust) connects to a thrust flattening at nearly 3 km depth, within the thick, fluid-rich poorly consolidated muddy Quaternary deposits of the Gutingkeng Formation which behave as an intermediate mechanical decoupling level (sections A-A' and B-B'). At greater depth (nearly 6 km) this thrust roots within a low-dipping decollement surface above the pre-Miocene basement. Section A-A' (Figure 5) additionally shows that the Tainan anticline corresponds to a small pop-up structure (line drawing in figure 5). This structure was previously identified on the basis of the radial centrifugal drainage pattern and the morphologic trace of the Houchiali Fault [*Sun*, 1964] but not interpreted in terms of deformation front.

The Chungchou anticline exhibits a morphological signature (Figure 4) which suggests a west verging asymmetric anticline. Its rectilinear western limit indicates that it is closely related to the motion of the Chungchou Fault, which also corresponds to a west vergent thrust flattening within the Gutingkeng Formation (Figure 5, section B-B'). The close spacing of the thrusts along the section is consistent with a shallow location of this intermediate decoupling level.

The Meilin thrust separates a slightly deformed western domain from an eastern domain characterized by well-expressed folds and faults (Figure 2). It probably corresponds to a steep thrust surface dipping toward the east, in relation to which a fault-propagation fold developed. At depth, however, the relation between the Meilin thrust and the décollement level is unclear; it is only tentatively extrapolated in section A-A'.

4.2.2. Takangshan and Panpingshan anticlines. The Takangshan and Panpingshan anticlines, trending NE-SW, provide good examples of fault-propagation folds commonly observed in southwestern Taiwan (Figure 2). The steeply dipping NW flanks of these anticlines are limited by NW vergent thrusts (such as the Meilin Fault), whereas their eastern flanks dip gently to the southeast.

Near the top of these anticlines, thick Pleistocene reefal limestones interbedded within the clastic layers of the Gutingkeng Formation crop out [e.g., *Heim and Chung*, 1962; *Chen et al.*, 1994]. The Takangshan and Hsiaokangshan reefs (T and H in Figure 2) are located on top of the Takangshan anticline, whereas the Panpingshan and Kaohsiung reefs (P and K on Figure 2) cover the top of the Panpingshan anticline. The age of the reefs ranges from 1.2 to 0.45 Ma and is younger from south (Kaohsiung) to north (Takangshan).

Tectonic analyses and paleostress reconstructions based on fault slip data and calcite twin data were carried out within the areas of the Takangshan and Panpingshan anticlines (Figures 2 and 8), especially in the reef material which is suitable for tectonic record. The reconstructed tectonic regimes and the corresponding data are briefly summarized in Figure 8. For details, refer to *Rocher et al.* [1996] and *Lacombe et al.* [1997].

In Panpingshan, normal faults trending N60°E to E-W and dipping gently to the north or steeply to the south revealed a NW-SE extension (Figure 8, diagram a at site 7). The σ_2 axis of the tensor is nearly parallel to bedding (hence to the anticline axis), while the σ_3 axis trends perpendicular to bedding strike. At least part of these normal faults developed contemporaneously with mud deposition and reef building [*Chen et al.*, 1994; *Lacombe et al.*, 1997]. We conclude that normal faulting was partly syndepositional and occurred during folding. In the Takangshan, Hsiaokangshan, and Kaohsiung reefs (Figure 2), some normal faults also indicate a WNW-ESE to NW-SE extension (Figure 8, diagrams c at site 5, b at site 6, and b at site 8).

Compressional features were also observed. In the Panpingshan quarry, left-lateral strike-slip faults trending N150°-160°E and right-lateral strike-slip faults trending N110°-130°E indicate a NW-SE compression (Figure 8, diagram b at site 7). This compression is perpendicular to the fold axis and related to folding. Two systems of large subvertical fractures were also measured; although striations are absent, they probably correspond to conjugate strike-slip faults related to a nearly E-W compression (Figure 8, diagram c at site 7). In site 8 a NW-SE compression has also been identified, marked in the field by both strike-slip and reverse faults (Figure 8, diagram a at site 8). A few tension gashes and strike-slip faults additionally indicate a N80°E compression (Figure 8, diagram c at site 8). In Hsiaokangshan most of the measured strike-slip faults are consistent with an E-W compression (Figure 8, diagram a at site 6). In Takangshan, two different systems of strike-slip faults could be identified. The first set is similar to the system of strike-slip faults identified in Hsiaokangshan and is also related to a nearly E-W compression (Figure 8, diagram a at site 5). The second set comprises conjugate right-lateral E-W strike-slip faults and left-lateral N160°E to N200°E strike-slip faults associated with N130°E trending tension gashes; these structures are consistent with a NW-SE compression (Figure 8, diagram b at site 5).

Closer inspection of the normal fault systems reveals a large dispersion in trend relative to the orientation of the fold axes; in detail, the normal fault sets include E-W trending and highly dipping faults, as well as nearly N-S to N40°E trending faults subparallel to bedding. Despite this azimuthal dispersion, the slips along these planes are mechanically consistent with a nearly NW-SE extension, which is the reason why they were not separated into subsets in Figure 8. This azimuthal dispersion could be tentatively related to the heterogeneity of the poorly lithified limestone material and/or to a gentle collapse (or differential compaction?) of the recently built, protruding coral reef on top of the poorly lithified mudstones. Rather, we consider that the E-W trending faults oblique at large angle to bedding are related to a nearly N-S extension, perpendicular to, and associated with, the E-W to WNW-ESE compression; the normal faults striking parallel to fold axis being related to local NW-SE extension in response to stretching at the hinge of the growing anticlines.

Relative chronology criteria, such as cross cutting relationships between faults, superimposed striations on fault surfaces, or attitude of minor structures and related paleostress axes with respect to fold axes and bedding provide constraints on stress evolution through time. In several cases, normal faults were reactivated as strike-slip faults under NW-SE (Figure 8, diagrams a and b at site 7) or E-W compressions (Figure 8, diagrams a and c at site 5). Concerning the compressions, diagrams a at site 5, a at site 6, c at site 7 and c at site 8 (Figure 8) show that the intersection of the conjugate families of strike-slip faults marking the E-W compression is vertical and that most striations on the fault planes are subhorizontal (and therefore less tilted than the bedding), so that this compression is likely to have prevailed after folding; in contrast, the NW-SE compression probably occurred during and after folding (Figure 8, diagrams b at site 5 and b at site 7

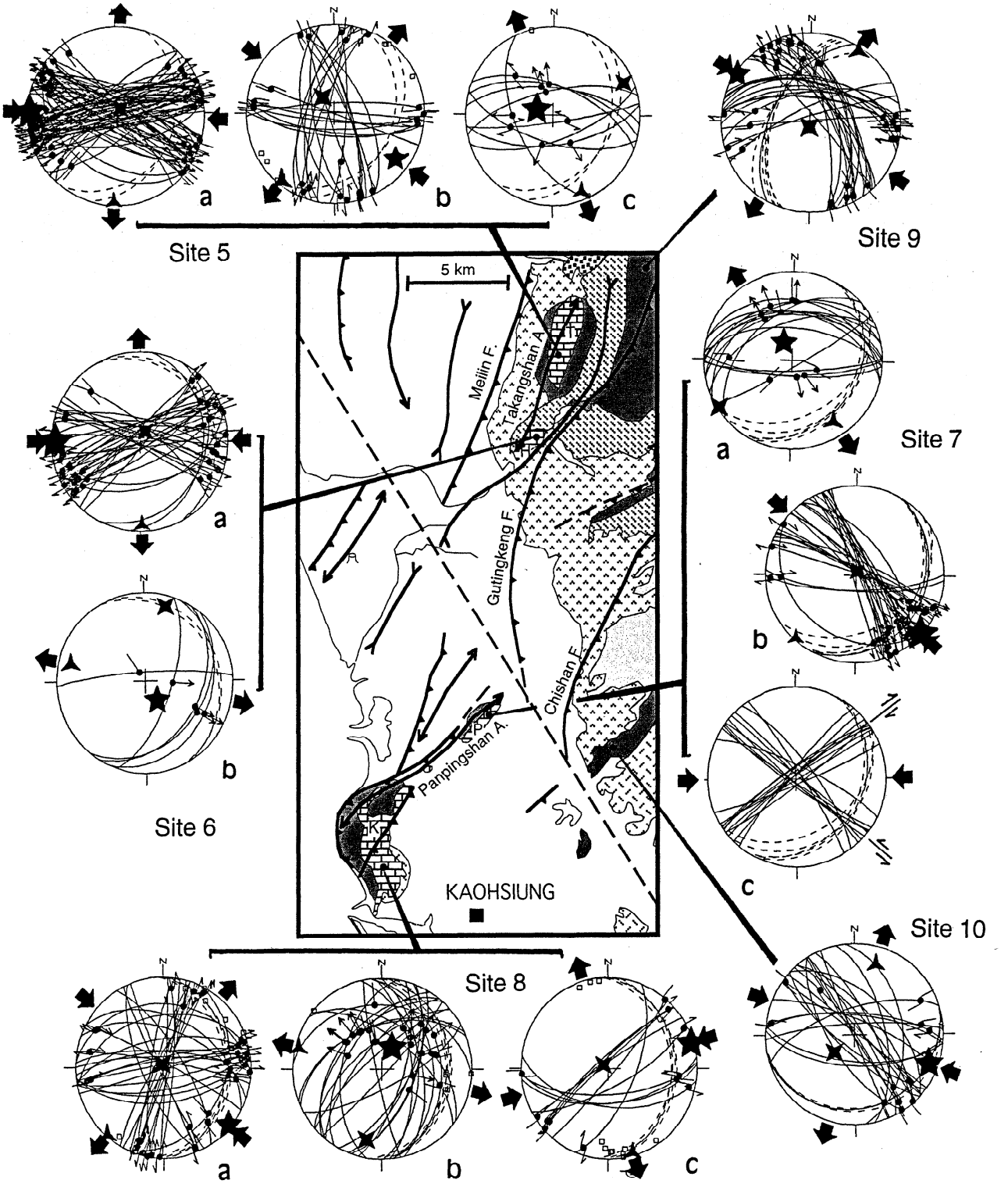

Figure 8. Results of stress reconstruction based on fault slip analysis in the vicinity of the Takangshan and Panpingshan anticlines. The map is part of that of Figure 2 (Longitude: 120°15'-120°25'; Latitude: 22°35'-22°55') and uses the same key as in Figures 2 and 7. Small open squares in diagrams represent poles to tension gashes.

and diagrams at sites 9 and 10). This suggests that the E-W compression postdated the NW-SE compression.

In summary, two compressional stress regimes have been identified: A NW-SE compression, followed by an E-W compression. The NW-SE compression is associated with the major stage of fold development and associated reef building; it is marked by strike-slip faults. Under this compression, early normal faults, sometimes syndepositional, locally developed in response to stretching at the hinge of the growing anticlines. The E-W compression mainly prevailed during the latest stages of folding; it is associated with a component of perpendicular N-S extension.

At the northeastern tip of the Takangshan anticline, microtectonic measurements were carried out in the Quaternary mudstones on the western side of the Guntingkeng Fault. In these mudstones, which display high dips to the west (65°-85°), conjugate strike-slip faults were observed, consistent with a N130° trending compression. These faults show non horizontal striations that dip more shallowly than bedding, which suggests that strike-slip faulting occurred during folding. The diagram at site 9 (Figure 8) illustrates the attitude of the fault set at a stage of limited back tilt, the calculated stress axes being horizontal (σ_1 and σ_3) and vertical (σ_2). This demonstrates the importance of the syn folding NW-SE compression in this area.

4.2.3. Fengshan anticline. The Fengshan anticline is one of the innermost features of the southwestern Taiwan Foothills (Figure 2). It bounds the Pingtung Plain to the west. The northern part of the Fengshan anticline trends N170°E to N-S. In the northern part of the fold most of the outcropping formations consist of the lower member of the Lingkou conglomerate (Figures 2 and 3).

To the south, the anticline axis turns from N-S to N110°E and becomes NE-SW where the anticline is covered by the Fengshan NN20 limestone. This limestone unconformably overlies the NN19 mudstones equivalent to the lower member of the Lingkou conglomerate [*Gong et al.*, 1996; this work]. Aerial photograph analyses suggest that this southern part is limited to the west by a west vergent thrust: the Fengshan Fault (section C-C'). Compressional features along the northern side of this thrust indicate that the NE oriented southern part has moved northwestward and has overthrust the N-S trending part of the fold. This may suggest a two-phase fold development.

Tectonic analyses of minor fault patterns have been performed in this fold (Figures 2 and 9). In its northern part, tension joints oriented N110°-120°E (Figure 9, diagrams at sites 11 and 12) probably mark a regional N110°-120°E strike-slip regime, consistent with the average trend of the Fengshan anticline. In site 13, E-W trending tension joints (Figure 9, diagram a at site 13) and normal faults (Figure 9, diagram b at site 13) are interpreted in terms of a NNE extension accompanying the WNW-ESE compression (σ_1-σ_2 stress permutation).

In the southern part of the anticline, a large quarry allows observation of the Fengshan reef limestone covering the crest of the anticline and its erosional contact with the underlying mudstones (Figure 10a). Calcite twin analysis reveals two states of stress: a NW-SE compression (with vertical σ_2 axis) as well as a NW-SE extension, consistent with those reconstructed in the other reef formations. In the mudstones, nearly E-W trending, low-dipping normal faults were predominantly observed (Figure 9, diagrams a and b at site 14 and Figure 10c), compatible with normal faults observed along the erosional contact between the limestones and the underlying mudstones (Figure 10b). On the highest part of the quarry a nearly E-W graben filled with limestone conglomerates shows channel-like sedimentary features (Figure 10d): It is bounded by normal faults associated with carbonate breccia, indicating that these normal faults acted as the graben filled up. The graben is sealed by continental red soils and conglomerates, whereas red clays have filled solution cavities developed within the limestone. These observations suggest that most extensional features prevailed during deposition of the upper part of the NN19 mudstones and building and emergence above sea level of the NN20 reef. Most normal faults trend E-W (Figure 9, diagram b at site 14); only few trend subparallel to bedding (Figure 9, diagram a at site 14). As already proposed by *Lacombe et al.* [1997] for the Takangshan and Panpingshan anticlines, the few normal faults parallel to fold axis are probably related to fold development, in response to tensional stresses initiated at the hinge of the growing anticline.

The WNW-ESE to E-W trending normal faults are tentatively interpreted in terms of extensional stresses perpendicular the WNW-ESE compression prevailing during and after folding in the Fengshan area. Some of these normal faults display evidence for a late reactivation as right-lateral strike-slip faults, consistent with a WNW-ESE directed compression (Figure 9, diagram c at site 14). We conclude that the WNW-ESE compression was responsible for both the development of the northern part of the Fengshan anticline and the associated fracturing (sites 11, 12, and 13) and the northwestward thrusting of its southern part (associated with reef building). This compression prevailed until recently after folding (site 14). In contrast to the clear contractional character of the NW-SE compression, the widespread occurrence of extensional features indicating a late N-S to NNE-SSW extension may reveal a situation of low N-S confinement during the recent WNW-ESE to E-W compression, a tectonic regime which may reflect the incipient tectonic escape in southwestern Taiwan (see section 6.3).

5. Geometry, Kinematics and Tectonic Significance of NW-SE Trending Fault Zones

5.1. Chishan Transfer Fault Zone (CTFZ)

Structural mapping reveals the existence north of our study area of a NW-SE structural trend, previously identified and called by *Deffontaines et al.* [1997] the Chishan Transfer Fault Zone (Figure 2), on both sides of which contrasting styles of deformation and mismatches of anticline axes occur. On the basis of new accurate analysis of DEM we propose that this zone extends farther west along the NW-SE branch of the Tsengwen river and accompanies the left-lateral offset of the deformation front to the north with respect to the frontal thrust of the Tainan anticline (Figure 2).

In the field the NW-SE Chishan Transfer Fault Zone (CTFZ) crops out as an elongated bulge, more than 20 km long and 1 km wide. This area contains several closely spaced NW-SE shear zones, associated with a variety of normal and reverse components of motion, along which most of the deformation has been accommodated. Wrench deformation zones are underlined in the field by highly deformed black clays which appear as black oblique stripes cutting through the light gray mudstones (Figure 11a). These sheets of highly sheared clays display narrow-spaced shear cleavages and small truncated elements, contrasting with the absence of large deformation in

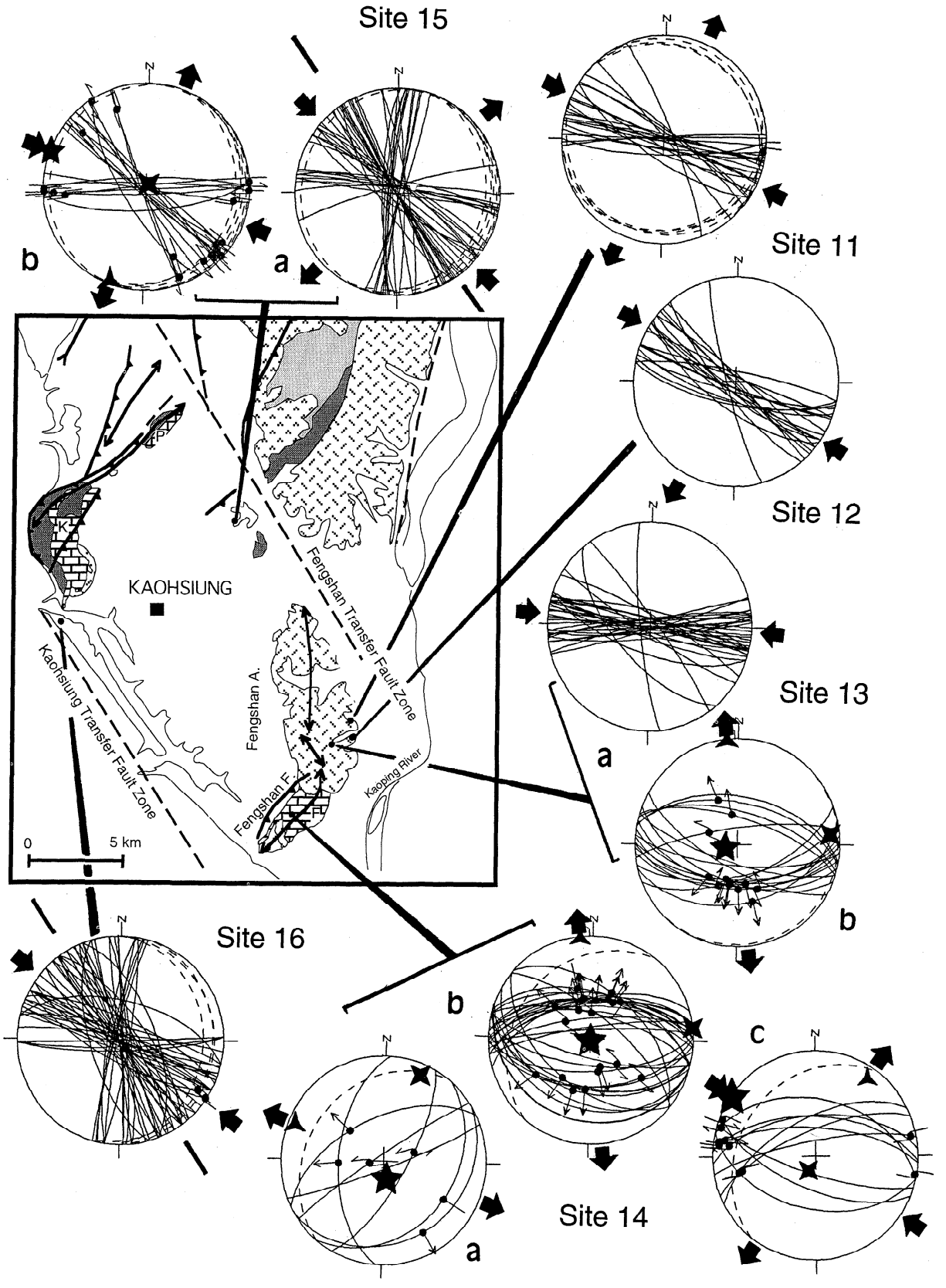

Figure 9. Results of stress reconstruction based on fault slip analysis within the Fengshan area. The map is part of that of Figure 2 (Longitude: 120°10'-120°25'; Latitude: 22°30'-22°45') and uses the same key as in Figures 2, 7, and 8.

A

B

Figure 10. Field observations from the Fengshan anticline. (a) Erosional contact between the Fengshan NN20 reef limestone and the underlying NN19 mudstones. (b) Normal faults along the erosional contact between the Fengshan reef limestones and the mudstones. (c) E-W trending syndepositional normal fault within the Fengshan mudstones. (d) E-W trending graben at the top of the Fengshan quarry. Cartoons provide simplified interpretations of photographs.

the surrounding mudstones (Figure 11a). The passive rotation and offsets of markers as well as S-C relationships within the shear bands consistently indicate a left-lateral sense of transpressive shear. At a wider scale the upward divergent geometry of these faults suggests that the whole pattern is a positive "flower structure", consistent with the wrench movement recognized in individual shear zones.

Microtectonic analyses carried out within the mudstones lead us to identify two systems of strike-slip faults (Figure 7). A N80°E compression is marked in the field by a system of conjugate left-lateral strike-slip faults trending N110°-120°E and right-lateral strike-slip faults trending N40°-60°E (Figure 7, diagram b at site 4, and Figure 11b). The striations on these fault planes lie within the bedding plane, and the intersection of the fault planes is not vertical; in addition, the σ_1 axis of the stress tensor is not horizontal, but is parallel to the dip direction of the beds, whereas σ_3 axis is parallel to the strike of beds. Back tilting fault slip data, hence the calculated stress axes, along the local strike of beds restores the initial attitude

C

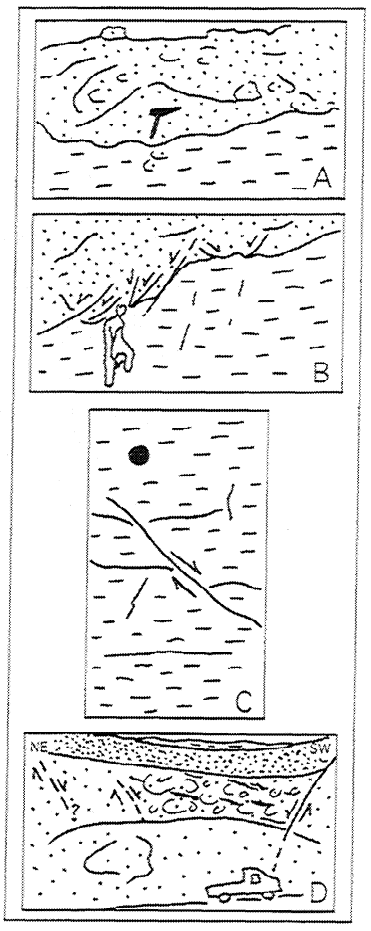

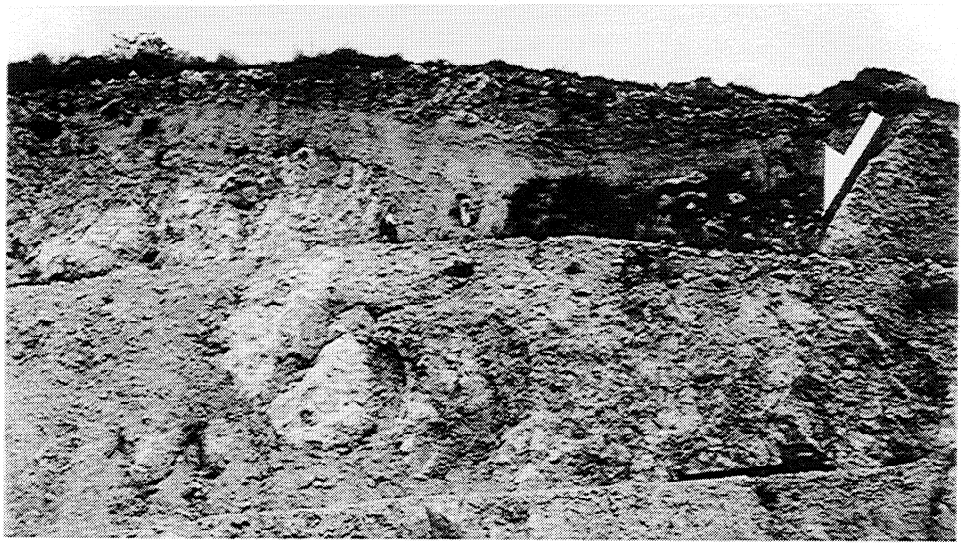

D

Figure 10. (continued)

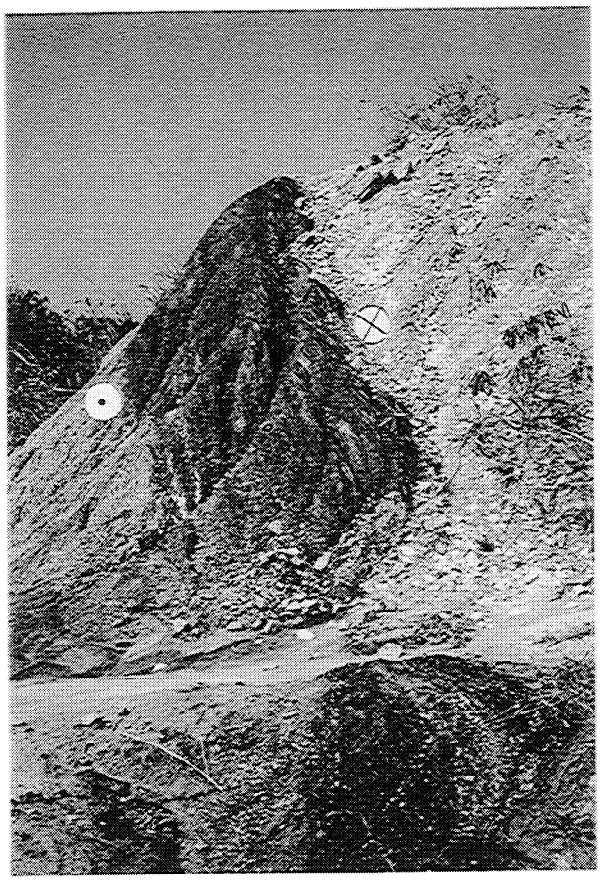

A

B

Figure 11. Field observations from the Chishan Transfer Fault Zone. (a) View of a NW-SE shear zone along the Chishan Transfer Fault Zone. The deformation zone is underlined by highly deformed stripes of black clays which cut and offset the light gray mudstones and show narrow-spaced shear cleavages. (b) Tilted set of minor conjugate N110°-120°E left-lateral and N40°-60°E right-lateral strike-slip faults observed within sandstones beds within the Chishan Transfer Fault Zone. Back tilting fault slip data along the local strike of beds restores the initial attitude of fault pattern; these are consistent with a σ_1 axis oriented N80°E and a σ_3 axis oriented N170°E (Figure 7, diagram b at site 4).

of fault pattern and stress axes (σ_1 and σ_3 axes horizontal), that is, a σ_1 axis trending N80°E and a σ_3 axis trending N170° (Figure 7, diagram b at site 4). This indicates that strike-slip faulting occurred probably in the earliest stage of folding, in response to N80°E compression. The second stress regime is marked by left-lateral strike-slip faults striking parallel to the NW-SE fault zone associated with conjugate right-lateral strike-slip faults trending N50°-80°E. Tensor determination [*Angelier*, 1984] indicates a N110°E compressional strike-slip stress regime (Figure 7, diagram a at site 4). Although the calculated σ_1 axis is nearly horizontal, the slip vectors on the strike-slip faults marking this compression display a variety of orientations, ranging from parallel to bedding to horizontal, which indicates that the N110°E compression probably prevailed before and after folding.

Both these stress orientations are similar to those identified away from the fault zone (Figure 7). Note that these stress regimes (and the related data subsets) were separated in the site considered on the basis of their relative chronology with respect to folding and of mechanical considerations (similar value of the acute angle between conjugate shear planes [*Anderson*, 1951]. If one accepts a dispersion of fault plane orientations, taking into account the dispersion range of stress orientations recognized away from the shear zone, both these fault systems can be gathered and accounted for by a single average N100°E compression.

Comparison between these reconstructed compressional trends and previous findings in the Foothills [*Angelier et al.*, 1986; *Chu*, 1990; *Lee*, 1994] leads us to conclude that at the regional scale the average N100°E compression probably reflects the Quaternary far-field state of stress. At the local scale, the occurrence of N80°E and N115°E compressions may be interpreted in terms of trend dispersion around a mean regional N100°E compression but it may also reveal occurrence of a regional N100°-110°E compression locally perturbed into a N80°E trend in the vicinity of the fault zone.

5.2. Fengshan Transfer Fault Zone (FTFZ)

Geomorphological and remote-sensing data combined with structural mapping emphasized the sigmoidal virgation and mismatches of most of the N20°-40°E trending thrusts and anticlines close the Fengshan N140°E Transfer Fault Zone inferred by *Deffontaines et al.* [1997](Figure 2). For instance, to the west the NE trending Chungchou thrust and the related anticline, as well as the Gutingkeng and the Chishan Faults, turn to the south and tend to become parallel to the N140°E direction (Figure 2). To the southeast the Fengshan anticline, which is oriented NE-SW to the south, turns to N-S close to the inferred fault zone (Figures 2 and 4). Cross sections of Figure 5 underline the slight difference in structural style between the sections A-A' and B-B' located north of the Fengshan Transfer Fault Zone (see section 5.4) and the section C-C'.

From a morphological point of view this fault zone has no clear straight surface expression: Its signature on the DEM (Figure 4) only consists of a roughly linear, NW-SE oriented depression zone. On the map of Figure 2 this subsiding area filled with Holocene deposist corresponds to the limit of the outcrops of Pleistocene Gutingkeng and Lingkou Formations. Few suitable outcrops are thus available along this inferred fault zone.One outcrop of Gutingkeng mudstones (Figure 9, site15) allowed measurements of striated faults and joint patterns. Four main sets of subvertical joints could be separated on the basis of the orientations of fracture planes: A dominant N120-150°E trending subset and second order subsets trending N-S, N100°E and N50°E. The geometry of the first three sets suggests that the N120°-150°E planes correspond to tension fractures, whereas N-S and N110°E fractures may correspond to conjugate shear fractures, all consistent with a NW-SE directed compression (Figure 9, diagram a at site 15). This is confirmed by observations of minor striated faults associated with joints, left lateral trending N130°-150°E and right lateral trending N090°-110°E, also consistent with a NW-SE compression (Figure 9, diagram b at site 15). The clustering of fracture orientations along the N140°E direction supports the occurrence of a major N140°E fault zone; the reconstructed N120°E compression indicates that this fault zone may have locally undergone a left-lateral motion.

5.3. Kaohsiung Transfer Fault Zone (KTFZ)

South of the Kaohsiung city and harbor, the rectilinear, NW-SE trending shape of the shoreline and the sigmoidal shape of the Shaoshan hill covered on its eastern side by the Kaohsiung limestone led *Deffontaines et al.* [1997] to suspect the occurrence of a NW-SE fault zone (Figure 2). New field observations carried out within the reef limestones on the southern part of the Kaohsiung harbor entrance, along the shoreline, enable us to discuss the probable existence of an offshore, nearly coast-parallel, fault zone. Tectonic measurements carried out on the coastline provide evidence that the local shape of the coast results from the occurrence of a dominant set of N125°-145°E large fracture planes. Despite dispersion (Figure 9, diagram at site 16), a clustering of fracture trends occurs along a N140°E direction, as noticed for the Fengshan Transfer Fault Zone. This dominant set of fractures forms a conjugate pattern with a minor set of N90°-110°E oriented fractures, suggesting that both sets originated in response to strike-slip fault regime, with σ_1 oriented N115°-120°E. This is confimed by numerous tension gashes, brecciated or filled with calcite, oriented N120°E, and by some evidence of left-lateral shear along N125°E directed planes interpreted as Riedel shears along a major N140°E fault zone. These field observations argue in favor of the existence of a major N140°E fault zone, with a possible left-lateral sense of motion.

5.4. Significance of the NW-SE Fault Zones

The interpretation of the Chishan, Fengshan, and Kaohsiung N140°E trending structures as transfer fault zones [*Deffontaines et al.*, 1997; this work] was based on the identification of thrust sheet segments displaying differential displacement / shortening on both sides of the fault zones. The sigmoidal shape of thrusts and fold axes, the contrasting styles and amplitude of deformation, the mismatches of compressional structures on both sides of the fault zone, as well as the different senses and rates of displacement between adjacent blocks argue in favor of transfer faulting. According to this interpretation these transfer fault zones are expected to trend approximately parallel (or oblique at small angle) to the direction of displacement of the tectonic units. The N140°E direction thus corresponds to the Quaternary regional direction of emplacement of tectonic units [*Mouthereau et al.*, 1996], slightly oblique to the direction of the reconstructed compressional trends (NW-SE and E-W).

The origin of such transfer fault zones deserves discussion. Experimental and analytical modelings coupled with field studies have resulted in a better understanding of the geometry

and mechanism of transverse zones [e.g., *Apotria et al.*, 1992; *Calassou et al.*, 1993; *Philippe*, 1994; *Baby et al.*, 1994; *Apotria*, 1995]. Such domains are characterized by structures oblique to the front belt. Sandbox modeling revealed that a thrust sheet moving over a décollement level may exhibit development of transverse structures in response to a lateral change in cover thickness due to basement geometry or basin boundary or to the lateral termination of the main décollement surface, which can be viewed as a high/low friction boundary. A primary tear fault may thus appear contemporaneously with fold-thrust development and be associated with a curvature of these structures as soon as they form; on both sides the amount of shortening is the same, but it may be accommodated in a different way. Such a system may secondarily evolve gradually into a transfer (or tear) fault, associated with a clear offset of already formed or currently forming folds. On both sides of the fault, differential displacement / shortening may be accommodated.

In Taiwan, the obliquity of the collision as well as the structural inhomogeneity of the Chinese margin colliding with the Luzon arc have played a major role in the structural style of the Foothills, resulting in an along-strike variation of thrust wedge geometry and kinematics of the frontal units [*Mouthereau et al.*, 1999a, b]. The precollisional structural pattern of the margin consists of a series of ENE oriented Miocene basins (e.g., the Tainan basin) and horsts resulting from the opening of the South China Sea, associated with NNW-SSE transfer faults. Revisited isobath maps of the top of the pre-Miocene rocks (Figure 12a) emphasize the occurrence of a major horst underlying the Taiwan Strait and the Coastal Plain: the Peikang High (Figure 1). Such a lateral change in basement geometry had a great influence on the geometry and kinematics of the west verging thrust sheets. Analogue modelings [*Lu et al.*, 1998] show that the Peikang High probably acted as a buttress for the west verging thrust units; the authors suggest that this structural high may have partially controlled the tectonic escape in southwestern Taiwan (see section 6.3) but also may have induced transfer zones in the frontal thrust belt. The influence of the basement on development of transfer zones has been highlighted for the Pakuashan Transfer Fault Zone [*Mouthereau et al.*, 1999c]: Detailled analyses have shown that the kinematic evolution of this area was, effectively, mainly controlled by the geometry of the Peikang High, acting as a buttress for the propagating thrusts; the Pakuashan transverse zone accommodated the motion of connected thrust sheets moving over an oblique ramp linked to the hinge fault of the Peikang High.

Immediately north of our study area, the Miocene Tainan basin underwent oblique inversion tectonics during the arc-continent collision, indicating that the basement was involved in collisional shortening [*Mouthereau et al.*, 1999a, b]. The southern limit of this area of basement-involved tectonics roughly corresponds to the Chishan Transfer Fault Zone (Figure 12b). Along this major boundary, probably inherited from the rifting period, an important lateral change of basement depth and thickness of Neogene sediments occurs (Figure 12b). This lateral change in the cover thickness probably localized a primary tear fault which accompanied thrust emplacement; this zone secondarily evolved into a transfer fault zone, on both sides of which largely contrasting styles of deformation occur. Field evidence additionally indicates local left-lateral wrench deformation, consistent with the regional stress field. At a broader scale this major fault zone is delineated by seismic activity and corresponds to the transition from subduction (or incipient collision) to the south to culmination of collision to the north. At the present-day this fault zone consists of a major crustal (lithospheric?) left-lateral wrench boundary, as suggested by earthquake focal mechanisms [*Yeh et al.*, 1991; *Rau and Wu*, 1998].

The Fengshan Transfer Fault Zone is clearly of second order compared with the Chishan Transfer Fault Zone. For this transfer fault zone, a primary tear fault nature can be proposed. Figure 12b shows no important change of Neogene deposit thickness beneath the inferred transfer zone. However, a slight change in basement topography, not visible at the scale of the section of Figure 12b, may have occurred, possibly across an inherited NNW-SSE transfer fault of the Chinese margin: Such a weakness zone in the basement may have localized such a primary tear fault in the cover. In contrast to the CTFZ this primary system has probably evolved poorly: The analysis of small-scale brittle deformation (Figure 9, site 15) suggests an incipient left-lateral component of strike-slip motion; consistent with the regional stress field, but the absence of clear straight signature of the fault zone at the surface and the lack of data do not allow us to draw definite conclusions.

6. Discussion and Conclusions

In this section, we aim at discussing the different possible interpretations concerning the relations in space and time and the genesis of tectonic structures within the outermost Foothills of the southwestern Taiwan belt and at placing the tectonic evolution of this key region within the framework of a lateral evolution from subduction (Manila trench) to oblique collision (prevailing in southern Taiwan).

6.1. Anticlines in Southwestern Taiwan: Tectonic or Diapiric?

Seismic surveys carried out offshore southwestern Taiwan have led to identification of mud diapirs [*Lee*, 1992; *Huang*, 1993; *Chang and Liu*, 1993]. These diapirs appear as elongated ridges running in a NNE-SSW direction, parallel to fold structures, faults, and diapir alignments observed on-land [*Sun and Liu*, 1993; *Liu et al.*, 1997]. These authors relate the diapiric movement to unbalanced loading caused by fast deposition of recent channel deposits along the syncline structures; they propose that faults alongside of the mud diapirs formed first in response to the Pliocene compression and later by the Pleistocene diapiric movement. The rapidly accumulated thick muddy sediments of the subsiding Taiwan foredeep provide a source material for these mud diapirs.

Such a diapiric origin has also been proposed for the on-land anticlines trending NE-SW in southwest Taiwan. As an example, *Wu* [1959] suggests that the lack of seismic reflectivity in the Panpingshan anticline reflects an intrusion of the mudstone of the lower member of the Gutingkeng Formation and concludes that the Panpingshan anticline is a diapiric structure. *Pan* [1968], *Hsieh* [1972] and *Huang* [1995] also consider the on-land Tainan, Chungchou, Panpingshan and Fengshan anticlines as mud diapiric anticlines.

These interpretations of the origin of on-land anticlines, according to which the driving mechanism is mud diapirism, do not account for the striking structural characteristics of the onland anticlines. Offshore, the elongated character of the ridges formed by diapir alignments argues in favor of a tectonic origin with initiation along NE trending folds and thrusts. Onshore, the general asymmetry of west vergent thrust-related anticlines (Figure 5), underlined by location of reefs on the eastern flanks of the folds [*Gong et al.*, 1996; *Lacombe et al.*, 1995, 1997] is difficult to explain through a simple model of mud diapirism, which usually results in more

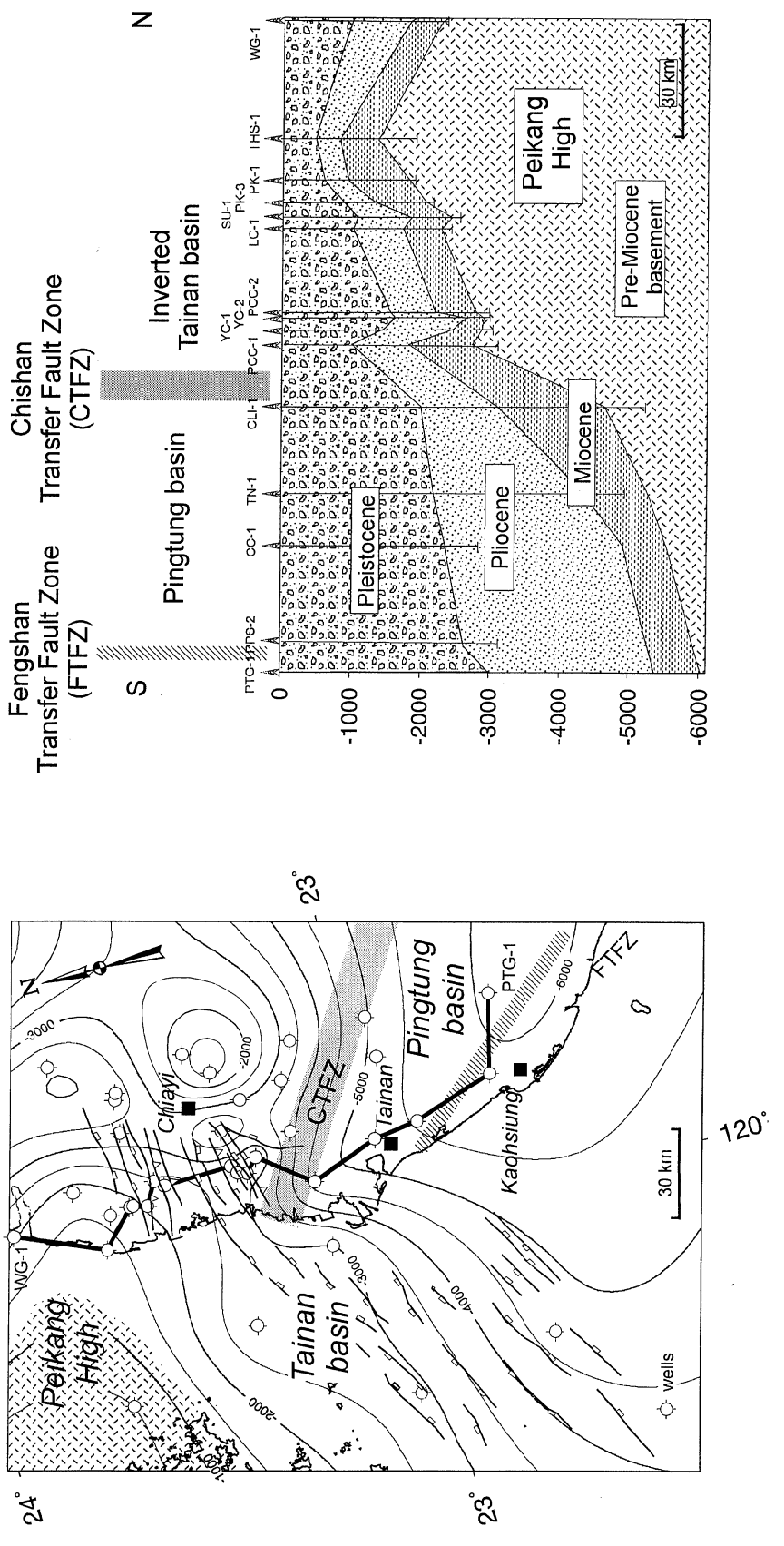

Figure 12. (a) Isobath map of the top of the pre-Miocene basement in southwestern Taiwan, based on correlation between well data [after *Mouthereau et al.*, 1999a, b]. Shaded areas show location of the Chishan and Fengshan Transfer Fault Zones (CTFZ and FTFZ). (b) Along-strike section showing the Neogene basins and highs along the profile connecting the wells of Figure 12a. Note (1) the location of the inverted Tainan basin on the southern edge of the Peikang High, and (2) the important change in basement geometry and Neogene deposit thickness across the CTFZ.

symmetric features. Furthermore, the regional consistency of the tectonic mechanisms and stress orientations identified within the fold structures indicate that onshore and offshore Taiwan the tectonic forces related to the Plio-Pleistocene collision are the major factor controlling structural evolution in this region.

As a consequence, mud diapirism is thought herein to be a second order phenomenon associated with folding and thrusting. Numerous mud volcanoes can be observed along major faults, such as the Gutingkeng and the Lungchuan Faults (Figure 2). This indicates that fluid and mud emergences are guided along major décollement and tectonic contacts, as commonly observed in subduction zones throughout the world (e.g., Barbados ridge [*Screaton et al.*, 1990; *Le Pichon et al.*, 1990; *Lallemant et al.*, 1990], and Nankai accretionary prism [*Henry et al.*, 1989]). Mud diapirism is basically initiated by upward migration of fluids and of fluid-saturated mud material in response to contraction due to thrusting and folding; a second possible step can be the enhancement of diapirism by loading of recent deposits over poorly consolidated muddy sediments [*Liu et al.*, 1997].

6.2. Reef Development in Southwestern Taiwan and Its Relation in Space and Time to Fold-and-Thrust Tectonics and Southward Propagating Collision

Recent papers provided significant results in terms of relationships between the reef limestones and the surrounding formations. *Chen et al.* [1994] demonstrated the conformable contact relationships between the early Pleistocene limestone of Panpingshan and the Gutingkeng Formation. *Gong et al.* [1995, 1996] emphasize some characteristics of these lenticular limestones, which are (1) rapid transition from underlying deep-water siliciclastic mudstones of the Gutingkeng Formation upward to reef limestones, (2) lateral interfingering with deep-water siliciclastics, and (3) no cover or else overlay by only terrestrial deposits, implying emergence above sea level since reef formation. These observations, as well as the close geographical relationship between reefs and anticlines and the results of tectonic analyses carried out within the reef limestones [*Lacombe et al.*,1995, 1997] have led to a model summarized below, which considers that reefs developed on structural highs raised by folding, on top of which decreasing clastic flow induced local favorable paleoecological environment for reef-building organisms.

According to this model, reefs developed on top of folds related to west vergent thrusts under a regional compressional stress. Continuing folding resulting from westward propagating thrusting allowed reef growth. During reef development, local syn folding extension may have occurred nearly perpendicular to fold axis, in response to tensile stresses at the hinge of the anticline. Additionally, an eastward migration of the climax of reef development is likely to have occurred at this stage because of the hinge migration and asymmetry of the fault-propagation fold, as well as some collapse along the eastern flank of the fold. Reefs developed until they reached water level and emerged. At this step, folding progressively slowed down and shortening in the reefs was achieved mainly by strike-slip faulting. Emergence of the reefs was accompanied by karst development (as observed in Takangshan and in Fengshan), marked by local dissolution of the limestones and deposition of red clays within cavities and former fractures.

If this model of tectonically controlled reef development is valid, the reefs are expected to provide time constraints on southwestward thrust migration. The relationship between the age of the reefs and the age of the thrust-related folds on the top of which they developed therefore needs a detailed discussion. The age of the reefs decreases northward, from Kaohsiung (middle NN19) to Panpingshan/ Hsiaokangshan (middle-late NN19) and to Takangshan (late NN19) (ages are after *Chang and Chi* [1983], *Chi* [1989] and *Lee* [1990]). Two hypotheses which may account for this age-spatial relationship are (1) a diachronic fold development from south to north during early Pleistocene times and a correlative thrust activation occurring later to the north (Takangshan and Hsiaokangshan) than to the south (Panpingshan and Kaohsiung), and/or (2) an uplift rate higher to the south than to the north. These hypotheses contradict somewhat the well-established southward migration through time of the Taiwan collision. According to a third hypothesis the age of the reefs may not exactly reflect the age of thrust development because in addition to the fold growth control on reef building, local changes of paleoecological environments in the foreland basin may also have occurred. In this latter case, the Meilin Fault, in relation to which the Takangshan and Panpingshan anticlines probably developed (Figure 2), would have initiated as early as 1 Myr ago, but lateral change in sedimentary conditions and paleoecological environments could have led to a reef development younger from south to north (from Kaohsiung to Takangshan). Sedimentary studies effectively suggest that the Tainan area was an early Pleistocene depocenter in the foreland basin [e.g., *Lin*, 1991]: This means that while sediments prograded the shoreline advanced toward the depocenter [*Gong et al.*, 1996], so that the favorable environmental conditions for reef building migrated with time from Kaohsiung to Takangshan (i.e., northward). This last hypothesis implies that the folds and associated NN19 reefs are accounted for by a single episode of thrust development around 1 Ma and that the time migration of reef development only reflects basin sedimentary dynamics.

Southwestern Taiwan also displays evidence for reef development younger than NN19. The Fengshan limestone and the Shaoshan limestone are dated NN20 (the latter cannot be shown at the scale of Figures 2 and 5). In contrast to the Takangshan, Hsiaokangshan, Panpingshan and Kaohsiung limestones both of them unconformably overlie the underlying formations: The folded Fengshan limestone is in erosional contact with the underlying gray siliciclastic mudstones, dated NN19, equivalent to the lowest member of the Lingkou conglomerates [*Chi*, 1979] (Figure 10a), whereas the non folded Shaoshan limestone unconformably overlies the Kaohsiung limestones and the Chichiao Formation (local equivalent of the upper Gutingkeng Formation, not distinguished in Figure 2). According to the model of reef development related to fault-propagation folds, the Shaoshan and Fengshan limestones probably formed in the same way. We consequently expect an episode of thrust-fold activation during the late Pleistocene, in agreement with the southward migration of the collision proposed by *Suppe* [1984] and in agreement with the two-phase fold development proposed for the Fengshan anticline.

Because of the more eastern location of the Fengshan anticline covered by the reefs with respect to the Kaohsiung area this late Pleistocene reef and fold development requires an out-of-sequence thrusting. A similar hypothesis can be drawn for the Shaoshan limestone which is located on the hanging-wall of the late high-angle reverse fault (the Shaoshan Fault) which cuts the eastern flank of the Panpingshan anticline, south of Kaohsiung (Figure 5, section C-C').

The unconformable overlay of the Kaohsiung limestones by the NN20 Shaoshan limestones, containing blocks of NN19 Kaohsiung limestones [*Sun*, 1963], may be interpreted either as resulting from the development of this reverse fault or in terms of slope-related deposition (talus deposit). The unconformable attitude of the Shaoshan limestones thus does not imply emergence of the Kaohsiung limestones and the Chichiao Formation above sea level and subsequent erosion. However, the unconformable attitude of the NN20 Fengshan limestone on the underlying NN19 mudstones (Figure 10a) needs explanation. As seen earlier, the southern Fengshan area provides evidence of a two-phase fold development, that is, the reactivation and the overthrust of the former Fengshan anticline. This implies that the deformed mudstones and the lower Lingkou conglomerates were (1) first folded and eroded during early Pleistocene times contemporaneously with the formation of the Panpingshan (and Takangshan?) anticlines, then (2) secondarily newly immerged (foreland subsidence of the Pingtung basin or sea level rise?) and (3) refolded, giving rise to reef development in southern Fengshan; this sequence of events may explain the erosional contact between reefs and underlying mudstones.

Summarizing, the age of the reefs in southwestern Taiwan (which ranges from nearly 1 Ma to 0.2 Ma), the location of these reefs on the top of anticlines, and the conformable or unconformable attitude of these reefs with respect to the underlying formations provide convincing evidence for two episodes of folding, during the early and late Pleistocene. However, two tectonic scenarios can be proposed: The first one relates the formation of the Takangshan and Panpingshan anticlines and the early folding in the Fengshan area to the same event, around 1 Ma, with a later reef development to the north in response to lateral variations of depositional environments within the foreland basin. This event would have been followed by out-of-sequence thrusting in southern Fengshan area (and possibly in the Shaoshan area), ~0.5 Myr ago. The second possible scenario relates the formation of the Panpingshan anticline and early folding in Fengshan area to the same event, associated with reef development at nearly 1 Ma; this event was followed by in-sequence thrusting, folding, and reef development in the Takangshan area at ~0.7-0.5 Myr, contemporaneous with out-of-sequence thrusting in southern Fengshan area.

6.3. Quaternary and Present-Day Stress and Strain Patterns and Tectonic Evolution of Southwestern Taiwan: Propagating Collision and Lateral Escape.

The synthesis of paleostress reconstructions carried out in Quaternary formations allows a tentative mapping of Quaternary σ_1 stress patterns in southwestern Taiwan (Figures 13a and 13b). A striking result of our study is that two compressional stress regimes have regionally prevailed. Despite difficulties in separation of data subsets and relative dating, we identified a NW-SE compression followed by a nearly E-W (WNW-ESE to ENE-WSW) compression. The first regime was clearly contractional and associated with the major stage of fold development, whereas the second regime generally prevailed during the latest stages of folding (at least south of the CTFZ) and was associated from north to south with an increasing component of perpendicular N-S extension; the related structures evolving southward from strike-slip and reverse faults north of Tainan (Figure 7) to strike-slip and normal faults in the Takangshan area (Figure 8) and to tension joints and normal faults in the Fengshan area (Figure 9).

These contrasting compressional trends, NW-SE and E-W on average, probably followed each other rapidly during the Pleistocene. They may reflect local changes in the kinematics of thrust units without any really significant change in the N309°E direction of plate convergence during the Pleistocene. This is confirmed by magnetic susceptibility anisotropy analyses which indicate that Quaternary deformation was dominated by an average N100°-110°E recent shortening [*Lee and Angelier*, 1995], nearly parallel to the average of the two Quaternary compressional trends (Figures 13a and 13b). This may indicate that in a setting of average regional N100°-110°E shortening, stresses are sensitive to slight changes in the kinematics of individual thrust sheets. However, relating precisely a given direction of stress to the Quaternary development and the kinematics of a given major structural unit still remains difficult: South of the CTFZ, the NW-SE compression was probably responsible for the major west-northwestward displacement of thrust sheets and related folding, whereas the late E-W compression only accompanied the latest stages of fold evolution and induced a late right-lateral/reverse motion along NNE thrusts. In contrast, north of the CTFZ, the NW-SE compression was not clearly identified, and folding was apparently mainly related to E-W to N100°E shortening (Figure 7).

The present-day kinematics and crustal strain distribution are documented by Global Positioning System data [*Yu and Chen*, 1992; *Yu and Kuo*, 1993; *Yu et al.*, 1995, 1997]. These data suggest that in contrast to the central part of the island where displacements of structural units are presently toward the WNW, the structural units of southwestern Taiwan are moving toward the WSW: This pattern of displacement velocities is illustrated by GPS displacement velocity vectors and trajectories of Figure 13d. This deflection of displacement trajectories has been interpreted in terms of a southwestward incipient tectonic escape in response to the ongoing WNW convergence, by comparison with the "so-called" concept of tectonic escape [*Sengör et al.*, 1985] or tectonic extrusion [*McKenzie*, 1972; *Tapponnier et al.*, 1983; *Ratschbacher et al.*, 1991] which is referred to the lateral motion of structural units toward a free boundary in response to collisional shortening. Analogue modeling experiments [*Lu and Malavieille*, 1994; *Lu et al.*, 1998] suggest that this lateral escape is greatly controlled by the structural inhomogeneity of the Chinese margin: The Peikang High probably acted as a buttress for the advancing thrust units, causing contraction against it and localizing a large dextral transfer zone around the shelf-slope break of the Chinese continental margin, along which the structures to the south were dragged to the southwest. Numerical modeling [*Hu et al.*, 1997] suggests that this escape may be enhanced by the decreasing confinement related to the Manila subduction zone.

Crustal strain orientations and magnitudes deduced from Global Positioning System data effectively indicate an average N110°E trending shortening, as well as a southward increasing magnitude of the perpendicular extension (Figures 13d and 13e, *Yu and Chen* [1996]) which probably reflects the southward escape. Concerning the present-day stress pattern, it is dominated by a N105°E compressional trend (Figure 13c) and is thus in good agreement with the present-day shortening; in this framework, local ENE-WSW oriented σ_{hmax} deduced from borehole breakouts [*Suppe et al.*, 1985] and ENE σ_1 trends deduced from earthquake focal mechanisms [*Yeh et al.*, 1991] (Figure 13c) could be partially interpreted as local stress reorientation at different depths of the present-day compression along NNE thrusts undergoing a right-lateral component of motion, consistent with the tectonic escape.

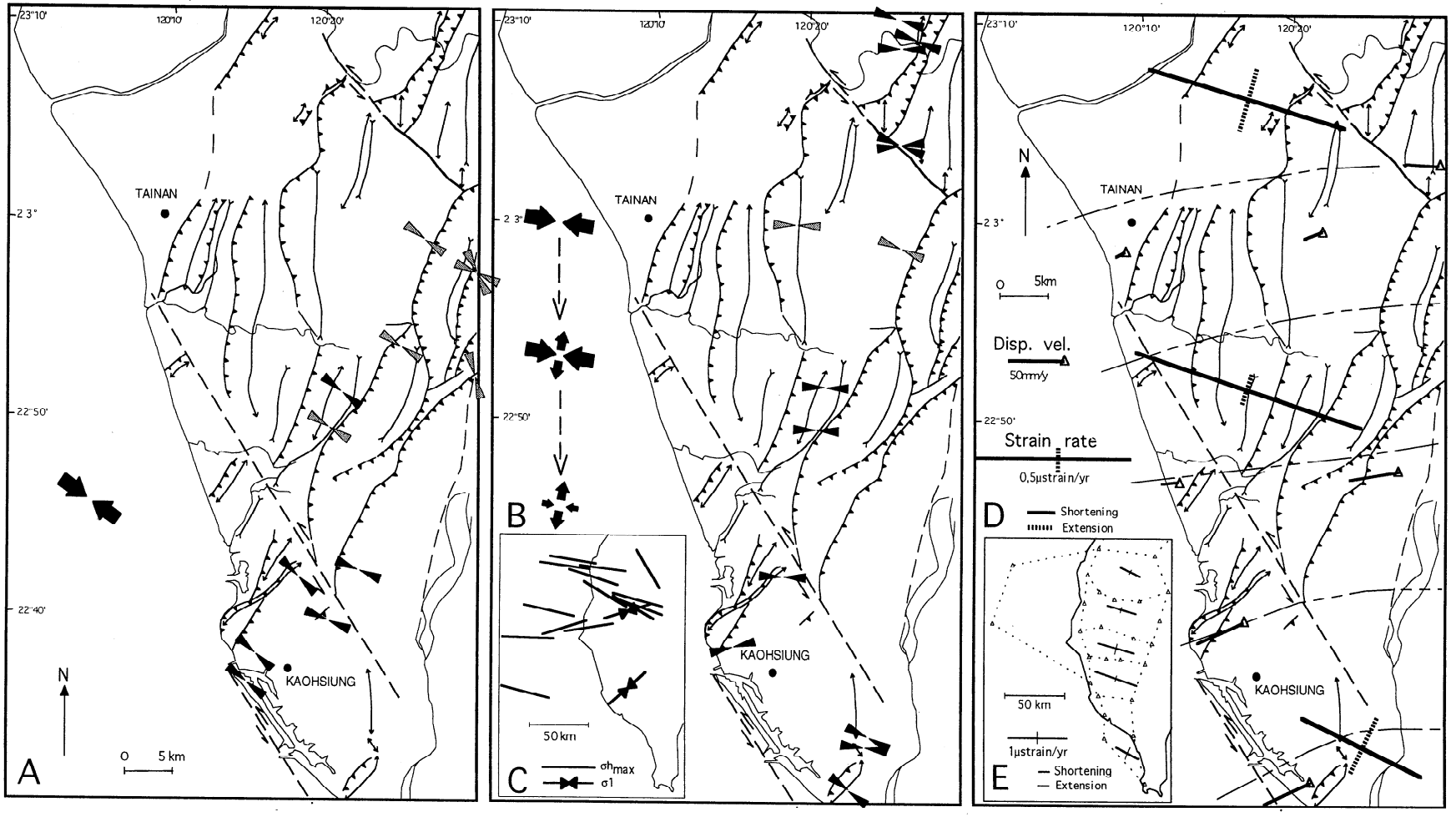

Figure 13. Pleistocene and present-day stress patterns and present-day crustal strain in southwestern Taiwan. Structural framework: same key as in Figure 2. (a) Pleistocene NW-SE compression. Convergent arrows indicate directions of σ_1 (shaded, data after *Rocher et al.*, [1996] and *Mouthereau et al.*, [1998]; solid, this work). The large solid convergent arrows indicate the average regional compression. (b) Late (?) Pleistocene WNW-ESE to E-W compression. Same key is used as in Figure 13a. Note the southward change in the relative stress magnitudes (convergent arrows, compression; divergent arrows, extension) accompanying the regional E-W regional compression. (c) Present-day stress pattern deduced from borehole breakouts (σ_{hmax})[*Suppe et al.*, 1985] and earthquake focal mechanisms (σ_1)[*Yeh et al.*, 1991]. (d) Displacement field and average principal strain rates in the area investigated. Triangles, GPS stations; heavy solid lines connected to triangles, displacement velocity vectors, with length proportional to velocity; dashed lines, extrapolated displacement trajectories from GPS stations. Note the southwestward present-day displacement, suggesting tectonic escape. Heavy lines, strain axes in the area investigated, length proportional to magnitude (see scale). (e) Average principal strain rates within Global Positioning System (GPS) subnets in southwestern Taiwan [*Yu and Chen*, 1996]. Triangles, GPS stations.

Comparison between Quaternary and present-day stress and strain patterns allows discussion of whether or not the kinematics of structural units has recently changed in southwestern Taiwan. It is clear that the E-W to WNW-ESE contraction prevailed both during the late Quaternary and at present-day. Is there evidence for a tectonic escape occurring (or beginning) during the Quaternary, and if so, is there any relation to the identified change in Quaternary stress regimes? The escape should have been accommodated by a Quaternary right-lateral component of motion along the southern edge of the Peikang High [*Lu and Hsü*, 1992; *Lu*, 1994; *Lu et al.*, 1998] and along the NNE trending thrusts on-land. This has been evidenced at the present-day from Global Positioning System data [*Angelier et al.*, 1999], but a clear component of right-lateral motion along on-land NNE thrusts during the Quaternary has never been clearly identified in the field, although suspected offshore southwestern Taiwan [*Liu et al.*, 1997]. The absence of clear signature of the tectonic escape in the on-land Quaternary deformation may be accounted for by a very recent beginning of this escape, which would have not markedly influenced the already existing structural pattern. However, the signature of the onset of tectonic escape may correspond to the change from the NW-SE to the nearly E-W (and locally ENE-WSW to NE-SW) compression, the latter being consistent with (or maybe resulting from) an incipient Quaternary right-lateral component of motion along NNE thrusts. Another possible signature could be the southward increasing occurrence of extensional features related to a nearly N-S Quaternary extension during the latest stage of (or after) fold development that we have documented in this paper. This along-strike change may indicate a southward decrease in N-S confinement, allowing σ_2/σ_1 stress permutations during the late E-W shortening. This is consistent with the present-day southward increase in extensional crustal strain relative to the regional N100°E shortening deduced from Global Positioning System (Figures 13d and 13e).

As a result, our structural and paleostress analyses provide a very efficient tool for deciphering the complex tectonic evolution of southwestern Taiwan: The results are in good agreement with the present-day stress-strain patterns and demonstrate that southwestern Taiwan is undergoing since the Pleistocene both a collisional shortening and an incipient lateral escape.

Acknowledgments. The work was supported by the French Institute of Taipei - National Science Council of Taiwan cooperation framework, by the Central Geological Survey of Taiwan, and by the Institut Français du Pétrole. The authors would like to thank A. Pfiffner and an anonymous reviewer for their constructive comments on the manuscript.

References

Anderson, E. M., The Dynamics of Faulting, 2nd ed., 206 pp, Oliver and Boyd, White Plains, N.Y., 1951.

Angelier, J., Tectonic analysis of fault slip data sets, *J. Geophys. Res., 89* (B7), 5835-5848, 1984.

Angelier, J., E. Barrier, and H. T. Chu, Plate collision and paleostress trajectories in a fold-thrust belt: The Foothills of Taiwan, *Tectonophysics, 125*, 161-178, 1986.

Angelier, J., S. B. Yu, J. C. Lee, J. C. Hu, and H. T. Chu, Active deformation of Taiwan collision zone: Discontinuities in GPS displacement field, paper presented at International Symposium on Subduction and Active collision in SE Asia, 4th Colloquium on Sino-French Cooperation Program in Earth Sciences, *Geol. Soc. of France*, Montpellier, 1999.

Apotria, T. G., Thrust sheet rotation and out-of-plane strains associated with oblique ramps: An example from the Wyoming salient, USA, *J. Struct. Geol.*, 17 (5), 647-662, 1995.

Apotria, T. G., W. T. Snedden, J.H. Spang, and D. V. Wiltchensko, Kinematic models of deformation at an oblique ramp. In *Thrust Tectonics*, edited by K.R. Mc Clay, pp 141-154, Chapman and Hall, New York, 1992.

Baby, P., M. Specht, J. Oller, G. Montemurro, B. Colletta, and J. Letouzey, The boomerang Chapare transfer zone (recent oil discovery trend in Bolivia): Structural interpretation and experimental appproach, In *Geodynamic Evolution of Sedimentary Basins*, edited by F. Roure et al., pp. 203-222, France, Technip, 1994.

Barrier, E., and J. Angelier, Active collision in eastern Taiwan: The Coastal Range, *Tectonophysics, 125*, 39-72, 1986.

Calassou, S., C. Larroque, and J. Malavieille, Transfer zones of deformation in thrust wedges: An experimental study, *Tectonophysics, 221*, 325-344, 1993.

Chang, S. S. L, and W. R. Chi, Neogene nannoplankton biostratigraphy in Taiwan and the tectonic implications, *Pet. Geol. Taiwan, 19*, 93-147, 1983.

Chang, C. H., and C. S. Liu, Mud diapirs in offshore southwestern Taiwan, paper presented at Annual Meeting, Geol. Soc. of China, Taipei, 1993

Chen, H. W., L. C. Wu, and H. H. Tsien, The contact relationship between the Early Pleistocene Panpingshan Limestone and Gutingkeng Formation in the Kaohsiung area, southern Taiwan (in Chinese), *Cent. Geol. Surv. Spec. Publ., 8*, 101-119, 1994.

Chi, L. M., Sedimentological study of limestones at southern Shaoshan, Kaohsiung (in chinese). M. Thesis, Nat. Sun Yat-Sen Univ., Kaohsiung, Taiwan, 1989.

Chi, W. R., A biostratigraphic study of the late Neogene sediments in the Kaohsiung area based on calcareous nannofossils, *Proc. Geol. Soc. China*, 22, 121-144, 1979.

Chinese Petroleum Corporation (CPC), Geological maps of Kaohsiung and Tainan, scale 1:100000, Taiwan, 1974.

Chu, H. T., Néotectonique cassante et collision plio-quaternaire à Taiwan, Ph.D. Thesis, *Mem. Sci. Terre, 90-28*, 292 pp, Univ. P. et M. Curie, Paris, 1990.

Deffontaines, B., J. C. Lee, J. Angelier, J. Carvalho, and J. P. Rudant, New geomorphic data on the active Taiwan orogen: A multisource approach, *J. Geophys. Res., 99* (B10), 20,243-20,266, 1994.

Deffontaines, B., O. Lacombe, J. Angelier, H. T. Chu, F. Mouthereau, C. T. Lee, J. Deramond, J. F. Lee, M. S. Yu, and P. M. Liew, Quaternary transfer faulting in Taiwan Foothills: Evidence from a multisource approach, *Tectonophysics, 274*, 61-82, 1997.

Etchecopar, A., Etude des états de contraintes en tectoniquc cassante et simulation de déformations plastiques (approche mathématique), Ph.D. Thesis, 270 pp., Univ. Sci. et Techn. du Languedoc, Montpellier, France, 1984.

Gong, S. Y., T. Y. Lee, J. C. Wu, S. W. Wang, and K. M. Yang, Possible links between Plio-Pleistocene reef development and thrust migration in the southwestern Taiwan, paper presented at International Conference and 3rd Sino-French Symposium on Active Collision in Taiwan, *Geol. Soc. of China*, Taipei, March 22-23, 1995.

Gong, S. Y., T. Y. Lee, J. C. Wu, S. W. Wang, and K. M. Yang, Possible links between the development of Plio-Pleistocene coral reef limestones and thrust migration in southwestern Taiwan, *J. Geol. Soc. China, 39* (2), 151-166, 1996

Heim, A., and C. T. Chung, Preliminary observations on the structure of the Kaohsiung limestone mountains, *Pet. Geol. Taiwan, 1*, 23-30, 1962.

Henry, P., S. Lallemant, X. Le Pichon, and S. Lallemand, Fluid venting along Japanese trenches: Tectonic context and thermal modelling, *Tectonophysics, 160*, 277-291, 1989

Ho, C. S., Geological map of Taiwan, scale 1:500,000, Cent. Geol. Surv., Minist. of Econ. Affairs, Taipei, 1986a.

Ho, C. S., A synthesis of the geologic evolution of Taiwan, *Tectonophysics, 125*, 1-16, 1986b.

Hsieh, S. H., Subsurface geology and gravity anomalies of the Tainan and Chungchou structures of the Coastal Plain of southwestern Taiwan, *Pet. Geol. Taiwan*, 10, 323-338, 1972.

Hu, J. C., J. Angelier, and S. B. Yu, An interpretation of the active deformation of southern Taiwan based on numerical simulation and GPS studies, *Tectonophysics, 274*, 145-169, 1997.

Huang, W. L., Distribution of mud diapirs offshore southwestern Taiwan, their relationships to the onland anticlinal structures and their effects on the deposition environment in southwest Taiwan (in Chinese), M. Thesis, Inst. Oceanogr., Nat. Taiwan Univ., Taipei, 1995.

Huang, Y. L., Analysis of geological structure in offshore southwestern Taiwan (in Chinese), M. Thesis, Nat. Taiwan University, Taipei ,1993.

Huiqi, L., K. R. McClay, and D. Powell, Physical models of thrust wedges. In *Thrust Tectonics*, edited by K. R. McKlay, pp. 71-81, Chapman and Hall, New York, 1992.

Lacombe, O., J. Angclier, and P. Laurent, Les macles de la calcite, marqueurs des compressions récentes dans un orogène actif: L'exemple des calcaires récifaux du sud de Taiwan, *C. R. Acad. Sci., Ser.II, 316*, 1805-1813, 1993.

Lacombe, O., J. Angelier, M. Rocher, H. W. Chen, H. T. Chu, B. Deffontaines, J. C. Hu, and J. C. Lee, Calcite twin analysis: A key to the recent stress fields at the front of the Taiwan Collision belt, paper presented at International Conference and 3rd Sino-French Symposium on Active Collision in Taiwan, *Geol. Soc. of China*, Taipei, March 22-23, 1995.

Lacombe, O., J. Angelier, H. W. Chen, B. Deffontaines, H. T. Chu, and M. Rocher, Syndepositional tectonics and extension-compression relationships at the front of the Taiwan collision belt: A case study in the Pleistocene reefal limestones near Kaohsiung,

SW Taiwan, *Tectonophysics, 274*, 83-96, 1997.

Lallemant, S., P. Henry, X. Le Pichon, and J. P. Foucher, Detailed structure and possible fluid paths at the toe of the Barbados accretionary wedge (ODP Leg 110), *Geology, 18*, 854-857, 1990.

Laurent, P., Les macles de la calcite en tectonique: Nouvelles méthodes dynamiques et premières applications, Ph.D. Thesis, 324 pp., Univ. Sci. et Techn. du Languedoc, Montpellier, France, 1984.

Lee, J. C., Structure et déformation active d'un orogène: Taiwan, Ph.D. Thesis, *Mem. Sc. Terre, 94-10*, 281 pp., Univ. P. et M. Curie, 1994.

Lee, T. Q. and J. Angelier, Analysis of magnetic susceptibility anisotropy of the sedimentary sequences in southwestern Foothills of Taiwan and its tectonic implications, paper presented at International Conference and 3rd Sino-French Symposium on Active Collision in Taiwan, *Geol. Soc. of China*, Taipei, March 22-23, 1995.

Lee, T. Y., Cenozoic plate reconstruction of southeast Asia and sequence stratigraphy and tectonics in the Tainan basin, offshore southwestern Taiwan, PhD Thesis, 240 pp., Univ. of Texas at Austin, 1992.

Lee, T. Y., Y. Y. Hsu, and C. H. Tang, Structural geometry of the deformation front between 22°N and 23°N and migration of the Penghu Canyon, offshore Southwestern Taiwan Arc-continent Collision Zone, paper presented at International Conference and 3rd Sino-French Symposium on Active Collision in Taiwan, *Geol. Soc. of China*, Taipei, March 22-23, 1995.

Lee, Y. H., Nannobiostratigraphy, age correlation and paleoenvironments of the limestones in Kaohsiung area (in Chinese), M. Thesis, Nat. Sun Yat-Sen Univ., Kaohsiung, Taiwan, 1990.

Le Pichon, X., P. Henry, and S. Lallemant, Water flow in the Barbados accretionary complex, *J. Geophys. Res., 95* (B6), 8945-8967, 1990.

Lin, D. S., Lithofacies and the sedimentary environment evolution of the Plio-Pleistocene series in the southwestern Taiwan Foothills region, M. Thesis, 93 pp., Nat. Taiwan Univ., Taipei, 1991.

Liu, C. S., I. L. Huang, and L. S. Teng, Structural features off southwestern Taiwan, *Mar. Geol., 137*, 305-319, 1997.

Lu, C. Y., Neotectonics in the foreland thrust belt of Taiwan, *Pet. Geol. Taiwan, 29*, 1-26, 1994.

Lu, C. Y., and K. J. Hsü, Tectonic evolution of the Taiwan Mountain belt, *Pet. Geol. Taiwan, 27*, 21-46, 1992.

Lu, C. Y., and J. Malavieille, Oblique convergence, indentation and rotation tectonics in the Taiwan Mountain belt: Insights from experimental modeling, *Earth Planet. Sci. Lett., 121*, 477-494, 1994.

Lu, C. Y., F. S. Jeng, K. J. Chang, and W. T. Jian, Impact of basement high on the structure and kinematics of the western Taiwan thrust wedge : insights from sandbox models, *Ter. Atm. Oc., 9* (3), 533-550, 1998.

McKenzie, D., Active tectonics of Mediterranean region, *Geophys. J.R Astron. Soc., 30* (2), 109-185, 1972.

Mouthereau, F., J. Angelier, B. Deffontaines, O. Lacombe, H. T. Chu, B. Colletta, J. Déramond, M. S. Yu, and J. F. Lee, Cinématique actuelle et récente du front de chaîne de Taiwan, *C. R. Acad. Sci., Ser.II, 323*, 713-719, 1996.

Mouthereau, F., J. Angelier, B. Deffontaines, S. Brusset, O. Lacombe, H. T. Chu, and J. Deramond, Folds and fault kinematics and tectonic evolution of the southwestern thrust belt of onshore Taiwan, paper presented at Annual Meeting, Geol. Soc. of China, Chungli, Taiwan, March 20-21, 1998.

Mouthereau, F., B. Deffontaines, O. Lacombe, and J. Angelier, Basement control on structural style, wedge geometry and kinematics at the front of the Taiwan mountain belt, paper presented at International Conference on Thrust Tectonics, *Royal Holloway Univ. of London*, April 26-29, 1999a.

Mouthereau, F., B. Deffontaines, O. Lacombe, and J. Angelier, Along-strike variations of the Taiwan belt front: Basement control on structural style, wedge geometry and kinematics, *Geol. Soc. Am Spec. Pub.*, 1999b (in press).

Mouthereau, F., O. Lacombe, B. Deffontaines, J. Angelier, H. T. Chu, and C. T. Lee, Quaternary transfer faulting and belt front deformation at Pakuashan (western Taiwan), *Tectonics, 18*, (2), 215-230, 1999c

Pan, Y. S., Interpretation and seismic coordination of the Bouguer gravity anomalies obtained in southern Taiwan, *Pet. Geol. Taiwan, 6*, 197-207, 1968.

Philippe, Y., Transfer zone in the southern Jura thrust belt (eastern France): Geometry, development and comparison with analogue modeling experiments, In *Hydrocarbon and Petroleum Geology of France*, edited by A. Mascle, *EAPG Spec. Publ. 4*, 327-346, 1994.

Ratschbacher, L., W. Frisch, H. G. Linzer, and O. Merle, Lateral extrusion in the Eastern Alps, 2, Structural analysis, *Tectonics, 10* (2), 245-256, 1991.

Rau, R. J., and F. T. Wu, Active tectonics of Taiwan orogeny from focal mechanisms of small-to-moderate-sized earthquakes, *Ter. Atm. Oc., 9* (4), 755-778, 1998.

Rocher, M., O. Lacombe, J. Angelier, and H. W. Chen, Mechanical twin sets in calcite as markers of recent collisional events in a fold-and-thrust belt: Evidence from the reefal limestones of southwestern Taiwan, *Tectonics, 15* (5), 984-996, 1996.

Screaton, E. J., D. R. Wuthrich, and S. J. Dreiss, Permeabilities, fluid pressures, and flow rates in the Barbados Ridge Complex, *J. Geophys. Res., 95*, 8997-9007, 1990.

Sengör, A. M. C., N. Görür, and F. Saroglu, Strike-slip faulting and related basin formation in zones of tectonic escape: Turkey as a case study, *SEPM Spec. Publ., 37*, 227-264, 1985.

Sun, S. C., The reef limestones and the geologic structures in the vicinity of Kaohsiung City, Taiwan, *Pet. Geol. Taiwan, 2*, 47-64, 1963.

Sun, S. C., Photogeologic Study of the Tainan-Kaohsiung Coastal Plain Area, Taiwan, *Pet. Geol. Taiwan. 3*, 39-51, 1964.

Sun, S. C. and C. S. Liu, Mud diapirs and submarine channel deposits in offshore Kaohsiung-Hengchun, southwest Taiwan, *Pet. Geol. Taiwan. 28*, 1-14, 1993.

Suppe, J., Kinematics of arc-continent collision, flipping of subduction, and back-arc spreading near Taiwan, *Mem. Geol. Soc of China., 4*, 67-90, 1984.

Suppe, J., C. T. Hu, and Y. J. Chen, Present-day stress directions in western Taiwan inferred from borehole elongation, *Petr. Geol. Taiwan. 21*, 1-12, 1985.

Tapponnier, P., A. Peltzer, Y. Le Dain, R. Armijo, and P. Cobbold, Propagating extrusion tectonics in Asia : new insights from simple experiments with plasticine, *Geology, 10*, 611-616, 1983.

Teng, L. S., Geotectonic evolution of late Cenozoic arc-continent collision in Taiwan: *Tectonophysics, 183*, 57-76, 1990.

Wu, C. S., Final report on seismic survey conducted on the Kaohsiung prospect, Taiwan, Int. Rep. Chinese Petroleum Corporation, 1959.

Wu, F., R. J. Rau, and D. Salzberg, Taiwan orogeny: Thin-skinned or lithospheric collision?, *Tectonophysics, 274*, 191-200, 1997.

Yeh, Y. H., E. Barrier, and J. Angelier, Stress tensor analysis in the Taiwan area from focal mechanisms of earthquakes: *Tectonophysics, 200*, 267-280, 1991.

Yu, S. B. and H. Y. Chen, A global positioning system network for crustal deformation study in Taiwan, *Bull. Inst. Earth Sci. Acad. Sinica, 12*, 52-55, 1992.

Yu, S. B. and H. Y. Chen, Spatial variation of crustal strain in the Taiwan area, paper presented at 6th Taiwanese Geophysical Meeting, *Univ. Chiayi*, Chiayi, November 1996.

Yu, S. B., and L. C. Kuo, Utilizing continuous GPS data for study the crustal deformation in Taiwan, *Bull. Inst. Earth Sci. Acad. Sinica, 13*, 77-82, 1993.

Yu, S. B., H. Y. Chen, and L. C. Kuo, Velocity field of GPS stations in the Taiwan area, paper presented at International Conference and 3rd Sino-French Symposium on Active Collision in Taiwan, *Geol. Soc. of China*, Taipei, March 22-23, 1995.

Yu, S. B., H. Y. Chen, and L. C. Kuo, Velocity field of GPS stations in the Taiwan area, *Tectonophysics, 274*, 41-59, 1997.

J. Angelier, B. Deffontaines, O. Lacombe, and F. Mouthereau, Département de Géotectonique, Université Pierre et Marie Curie, T26-25, E1, Boîte 129, 4 place Jussieu, 75252 Paris Cedex 05, France. (olivier.lacombe@lgs.jussieu.fr)

H.T. Chu, Central Geological Survey, MOEA, P.O. Box 968, Taipei, Taiwan. (chuht@linx.moeacgs.gov.tw)

C.T. Lee, Institute of Applied Geology, National Central University, Chungli, Taiwan. (ct@gis.geo.ncu.edu.tw)

(Received December 10, 1998;
revised May 6, 1999;
accepted May 27, 1999.)